PHOENIX INTERFEROMETER

Paul G. J. Morse

Block Engineering, Incorporated

Prepared for:

Air Force Avionics Laboratory
Advanced Research Projects Agency

June 1975

AFAL-TR-75-94

PHOENIX INTERFEROMETER

Block Engineering, Inc.
19 Blackstone Street
Cambridge, Massachusetts 02139

June 1975

TECHNICAL REPORT AFAL-TR-75-94

Final Report for Period December 1973 - January 1975

Approved for Public Release; distribution unlimited

Prepared for
Advanced Research Projects Agency
1400 Wilson Boulevard
Arlington, Virginia 22209

Air Force Avionics Laboratory
Air Force Systems Command
Wright-Patterson Air Force Base, Ohio 45433

NOTICE

When Government drawings, specifications, or other data are used for any purpose other than in connection with a definitely related Government procurement operation, the United States Government thereby incurs no responsibility nor any obligation whatsoever; and the fact that the government may have formulated, furnished, or in any way supplied the said drawings, specifications, or other data, is not to be regarded by implication or otherwise as in any manner licensing the holder or any other person or corporation, or conveying any rights or permission to manufacture, use, or sell any patented invention that may in any way be related thereto.

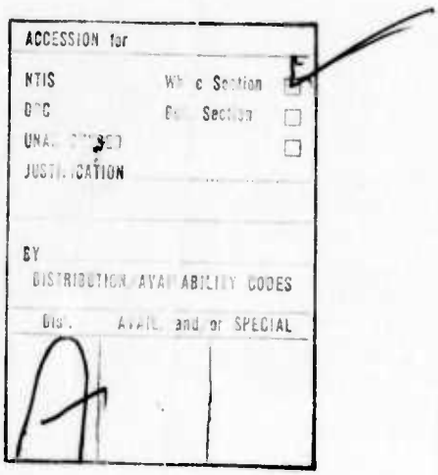

Copies of this report should not be returned unless return is required by security considerations, contractual obligations, or notice on a specific document.

UNCLASSIFIED

SECURITY CLASSIFICATION OF THIS PAGE (When Data Entered)

REPORT DOCUMENTATION PAGE		READ INSTRUCTIONS BEFORE COMPLETING FORM
1. REPORT NUMBER AFAL-TR-75-94	2. GOVT ACCESSION NO.	3. RECIPIENT'S CATALOG NUMBER
4. TITLE (and Subtitle) PHOENIX INTERFEROMETER		5. TYPE OF REPORT & PERIOD COVERED Final Technical Report December 1973-January 1975 6. PERFORMING ORG. REPORT NUMBER
7. AUTHOR(s) Paul G.J. Morse		8. CONTRACT OR GRANT NUMBER(s) F33615-74-C-1074
9. PERFORMING ORGANIZATION NAME AND ADDRESS Block Engineering, Inc 19 Blackstone St. Cambridge, MA 02139		10. PROGRAM ELEMENT, PROJECT, TASK AREA & WORK UNIT NUMBERS 62204F 7660 01 13
11. CONTROLLING OFFICE NAME AND ADDRESS ARPA/STO 1400 Wilson Blvd. Arlington, VA 22209		12. REPORT DATE June 1975 13. NUMBER OF PAGES 74 77
14. MONITORING AGENCY NAME & ADDRESS (if different from Controlling Office) AF Avionics Lab/RWC Air Force Systems Command Wright-Patterson AFB, OH 45433		15. SECURITY CLASS. (of this report) UNCLASSIFIED 15a. DECLASSIFICATION DOWNGRADING SCHEDULE

16. DISTRIBUTION STATEMENT (of this Report)

Approved for Public Release; distribution unlimited.

17. DISTRIBUTION STATEMENT (of the abstract entered in Block 20, if different from Report)

18. SUPPLEMENTARY NOTES

19. KEY WORDS (Continue on reverse side if necessary and identify by block number)

Infrared, Spectrometer, Interferometer, Spectroscopy, Radiance, Plumes, Airborne Sensor, IR Sensor, Fourier Transform Spectroscopy

20. ABSTRACT (Continue on reverse side if necessary and identify by block number)

The design and fabrication of a SWIR replacement interferometer head for the Firebird Interferometer System is described. The original Firebird system included a cryogenic LWIR Fourier interferometer in a stabilized tracking mount on a U-2 aircraft

DD FORM 1 JAN 73 1473 EDITION OF 1 NOV 65 IS OBSOLETE

UNCLASSIFIED

SECURITY CLASSIFICATION OF THIS PAGE (When Data Entered)

Block 20 Continued

for making measurements on high altitude plumes. The SWIR replacement, cooled to 250°K has a maximum spectral resolution of 0.6cm^{-1} in the 2-5.5μm region. The field of view is 5 - 6 mrdn and the diameter of the collecting optics is 4". The instrument is cooled by passing boil-off nitrogen from the LN_2 reservior through the insulated vessel about the interferometer.

The only change to the Firebird system needed to accommodate the new sensor is the replacement of several circuit boards. No hard wiring or plumbing changes are required, thus making the replacement readily reversible.

The interferometer has been tested and meets all specifications, with the exception of the NESR, which is a factor of three greater than it should be.

FOREWORD

This report describes work performed by Block Engineering, Inc., 19 Blackstone St., Cambridge, MA 02139, under Contract # F33615-74-C-2142. The objective of this effort was the design and fabrication of a SWIR replacement sensor for the Firebird Interferometer System, fabricated under Contract # F33615-72-C-1074. The SWIR sensor was successfully completed and integrated into the Firebird system. The project engineer was R.B. Sanderson, AFAL/RWC.

This program was a joint effort, supported in part by the Advanced Research Projects Agency under Project 2116 and in part by the AF Avionics Laboratory under Project 76600113. The original Firebird contract was supported by ARPA Project 2116 and AFAL Project 7660112. The final report for this effort has been published as AFAL TR-79-340. Aircraft modifications and fabrication of a LLLTV acquisition and tracking system were performed under AFAL Project 76600114 and are described in AFAL TR-74-247. Research was performed during the period July 1972 - June 1974 and the report was submitted in August 1974.

TABLE OF CONTENTS

LIST OF ILLUSTRATIONS

LIST OF ILLUSTRATIONS

SUMMARY

Under Contract No. F33615-74-C-1074, Block Engineering, Inc., Cambridge, Massachusetts was contracted to design, develop, fabricate, and test an airborne, high resolution interchangeable short wavelength infrared (SWIR) spectrometer for use with the Firebird system previously constructed under Contract No. F33615-72-C-2142.

The primary objective of the program was to provide a short wavelength spectroscopic capability to the Firebird system. The extension to shorter wavelengths permits acquisition of high resolution data in the important 2.7 and 4.2 micron regions. This information is considered essential for the development of plume radiation models and the unambiguous identification of specific excitation mechanisms in the SWIR spectral region.

The spectrometer to be built for this program was to utilize a rapid scanning, high spectral resolution Michelson interferometer operating at high altitude ambient temperatures, around 220°K. The sensor was to have a spectral range of 2 - 5.5 microns and a field of view of 5.6 milliradians which could be pointed at or held on airborne targets by means of the Firebird stabilized tracking system. The sensor was to be a direct replacement for the long wavelength infrared (LWIR) Firebird sensor with a minimum of changes to the remaining Firebird system components to insure optimum sensor interchangeability.

The interferometer spectrometer was designed, developed, and fabricated at the contractor's facilities in Cambridge, Massachusetts. The sensor met or exceeded all design specifications with the exception of the sensitivity requirement. Failure to meet sensitivity specifications was attributed to unusually high detector noise mechanisms limiting the sensitivity improvement under reduced background conditions, fully discussed in Section VI.

SECTION I

INTRODUCTION

1.0 Program Background

The purpose of this program was to design and fabricate an airborne, high resolution, high sensitivity interferometer head operating in the 2 - 5.5 micron spectral region. The sensor, cooled to ambient temperature at altitude, provides a short wavelength spectroscopic capability to the Firebird interferometer system developed by Block Engineering, Inc. for the Air Force under a previous contract, #F33615-72-C-2142. It is expected that data obtained from the SWIR sensor will help resolve questions concerning plume radiation mechanisms and specific radiating species in the important 2.7 and 4.2 micron regions.

The design and construction of the interferometer spectrometer is basically similar to the rapid scanning LWIR Michelson interferometer constructed for the Firebird program. The use of modern rapid scanning interferometers to obtain spectral distributions of various sources is rapidly supplanting the application of grating and other instrument types because of the inherent spectral precision in difficult environments, since all wavelengths act simultaneously to produce the signal, and complete high resolution spectral information is obtained in a fraction of a second. Block has developed an extremely rugged version of the rapid scanning Michelson interferometer in its Model 197 unit that has operated successfully in various configurations from 77°K to 327°K, in vacuum and under atmospheric conditions of up to 100% relative humidity, with spacecraft launch, aircraft and helicopter field environments applicable. This unit formed the basis of both the Phoenix and Firebird sensors.

This report presents a summary of the completed 13 month

activity by Block Engineering to construct and successfully test the Phoenix spectrometer system for the Air Force Avionics Laboratory, Wright-Patterson Air Force Base.

SECTION II

SYSTEM DESIGN

2.0 General

The primary objective of the Phoenix spectrometer program was to provide a short wavelength spectroscopic capability to the Firebird system. The extension of the Firebird system to shorter wavelengths was achieved by constructing a replacement high resolution interferometer head operating in the 2 - 5.5 micron wavelength region near ambient temperature at altitude and by appropriately modifying the ground based Firebird data system. The substitution required only minor reversible modifications to the remaining Firebird sub-systems to accomodate the higher electrical frequencies and the less stringent cooling needs of the SWIR sensor.

The following list of design specifications define in detail the stated objectives for the complete Phoenix program. All of the specification requirements were met by the Phoenix sensor which was ultimately fabricated and delivered, with the exception of certain performance specifications for the interferometer noted in this report.

2.1 Design Specifications

Required Components

The Phoenix system shall include:

a) Sensor Head
- Telescope
- Interferometer
- Sensor cooling system

b) Modification kit consisting of
- Complete set of sensor control electronics compatible with the Firebird measurement system.

- Modifications to the remaining Firebird subsystems as necessary to insure proper sensor operation.

Major Functional Requirements

Sensor Head

Collecting Optics

a) Pointing range: pitch ± 30°, roll ± 10° from zenith

b) Aperture: 4" diameter minimum full aperture

c) Field of view: 5.6 mrad full angle

d) Operating temperature: 220°K as a design goal

Interferometer

a) Spectral range: 2 - 5.5 microns

b) Spectral resolution: 0.7 cm^{-1}

c) Wavenumber precision: 0.1 cm^{-1}

d) Spectral scan rate: 3 scans/sec

e) Operating temperature: 250°K maximum with 220°K as a design goal

f) Sensitivity: NESR (2μ) = 4×10^{-9} $w/cm^2\text{-ster-}cm^{-1}\text{-scan}$
NESR (4μ) = 2×10^{-9} $w/cm^2\text{-ster-}cm^{-1}\text{-scan}$

Specified Components

a) A reference interferometer shall be used to accurately measure the moving signal mirror position and velocity.

b) Full internal radiance calibration capability shall be supplied.

c) A window over the telescope aperture shall be provided.

d) The telescope shall be equipped with a retractable capping mechanism to protect optics from sea level ambient water vapor environment.

2.2 Design Approach

2.2.1 General System Description

The Phoenix spectrometer package consists of a replacement high resolution, high sensitivity interferometer head operating in the 2 - 5.5 micron spectral region near ambient temperature at altitude (220°K). In addition to the sensor head, the Phoenix system also includes a set of plug-in printed circuit cards which provide unique control of the sensor via the Firebird main frame electronics.

The integration of the sensor unit with the Firebird system occurs solely at the gimbal interface. Mechanically, the sensor mounts to the gimbal structure in a manner similar to its Firebird counterpart. The sensor mass is essentially identical to that of the LWIR sensor, eliminating any requirement for gimbal servo loop optimization with each head interchange. In addition, the electrical and cryogenic interfaces at the gimbal site require no modification since the electrical wiring and plumbing external to the sensors remain intact; see Figure 1.

The operation of the replacement sensor head is monitored and controlled via the 3 control panels provided with the Firebird system. These controls include internal heater controls, interferometer controls, and telescope door controls as well as several key component status lights and an output signal monitoring meter. Preflight system verification is accomplished through the Firebird ground support equipment package which retains its versatility in the Phoenix configuration. The package displays all instrument parameters for quick operator inspection.

Although the sensor units are similar in many respects, due to the different wavelength coverage, the SWIR sensor differs substantially in several areas particularly in the signal frequencies generated and the less stringent cooling needs

2.2 Design Approach

2.2.1 General System Description

The Phoenix spectrometer package consists of a replacement high resolution, high sensitivity interferometer head operating in the 2 - 5.5 micron spectral region near ambient temperature at altitude (220°K). In addition to the sensor head, the Phoenix system also includes a set of plug-in printed circuit cards which provide unique control of the sensor via the Firebird main frame electronics.

The integration of the sensor unit with the Firebird system occurs solely at the gimbal interface. Mechanically, the sensor mounts to the gimbal structure in a manner similar to its Firebird counterpart. The sensor mass is essentially identical to that of the LWIR sensor, eliminating any requirement for gimbal servo loop optimization with each head interchange. In addition, the electrical and cryogenic interfaces at the gimbal site require no modification since the electrical wiring and plumbing external to the sensors remain intact; see Figure 1.

The operation of the replacement sensor head is monitored and controlled via the 3 control panels provided with the Firebird system. These controls include internal heater controls, interferometer controls, and telescope door controls as well as several key component status lights and an output signal monitoring meter. Preflight system verification is accomplished through the Firebird ground support equipment package which retains its versatility in the Phoenix configuration. The package displays all instrument parameters for quick operator inspection.

Although the sensor units are similar in many respects, due to the different wavelength coverage, the SWIR sensor differs substantially in several areas particularly in the signal frequencies generated and the less stringent cooling needs

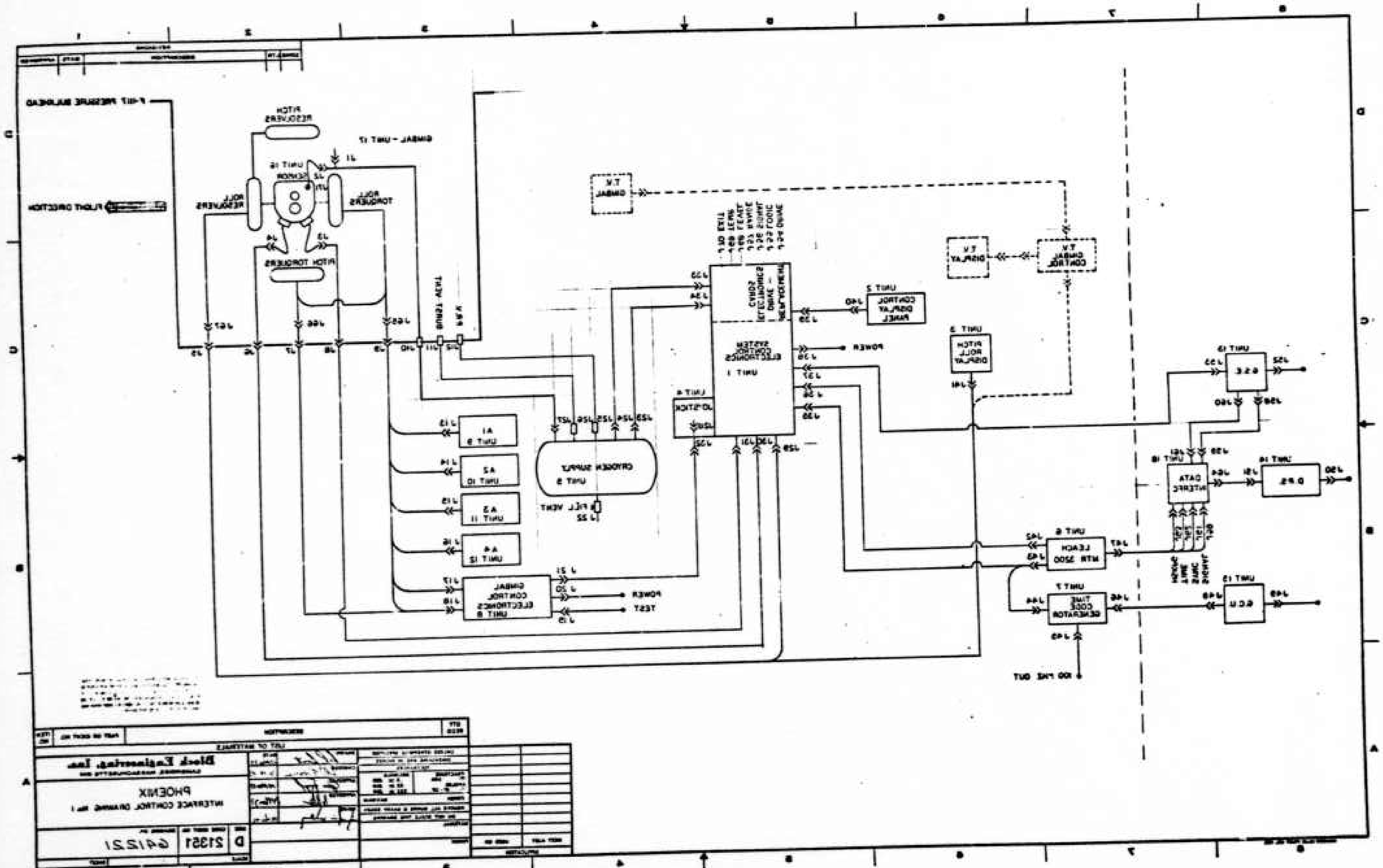

F-111 PRESSURE BULKHEAD
FLIGHT DIRECTION
PITCH RESOLVERS
ROLL RESOLVERS
ROLL TORQUERS
PITCH TORQUERS
UNIT 16 SENSOR
GIMBAL - UNIT 17
BURST VENT
FILL VENT
CRYOGEN SUPPLY UNIT 5
A1 UNIT 9
A2 UNIT 10
A3 UNIT 11
A4 UNIT 12
GIMBAL CONTROL ELECTRONICS UNIT 8
POWER
TEST
JOYSTICK UNIT 4
SYSTEM CONTROL ELECTRONICS UNIT 1
CARDS ELECTRONICS DRIVE - NEWLOCK...
J40 EXIT
J89 TEMP
J89 FEAST
J27 RANGE
J26 SIGNAL
J25 LOGIC
J24 DRIVE
CONTROL DISPLAY PANEL UNIT 2
PITCH ROLL DISPLAY UNIT 3
T.V GIMBAL
T.V DISPLAY
T.V GIMBAL CONTROL
LEACH MTR 3200 UNIT 6
TIME CODE GENERATOR UNIT 7
100 PHZ OUT
DATA INTERFC UNIT 18
O.S.E. UNIT 13
D.P.S. UNIT 14
E.C.U. UNIT 15
Block Engineering, Inc.
PHOENIX
INTERFACE CONTROL DRAWING No. 1
D 21351 641221
LIST OF MATERIALS

required; see Table 1 for a complete list of system specifications for the Phoenix sensor. These differences make it necessary to modify certain Firebird subsystems to accomodate the Phoenix sensor. Electrically the changes consist of the removal and substitution of appropriate printed circuit cards in the main frame electronics. These cards provide unique control for each system and will not require adjustment when sensors are interchanged. In addition to these reversible modifications, the successful integration of the Phoenix sensor with the Firebird system required that a once only modification be implemented on the ground-based Firebird data processing subsystem to accomodate the higher electrical frequencies generated by the Phoenix sensor. The modification, carried out at the contractor's facilities, consisted of changing the original 15 bit A/D convertor to a 12 bit machine. The 12 bit A/D has a faster conversion time per input data point, increasing the sampling rate capability of the system from 20 KHz to 100 KHz.

To achieve the high detector sensitivity required for the Phoenix sensor, it is necessary to reduce the optics photon noise below intrinsic detector preamplifier noise. This objective is accomplished by reducing the temperature of the spectrometer sufficiently so that the remaining background signal and noise comes from atmospheric radiation. Since the contribution to noise of an instrumental background at 220°K is reasonably small in the 2.0 to 5.5 micron region, the Phoenix sensor need not be cooled to the extremely low temperatures constraining the LWIR sensor. This reduction in cooling complexity results in a relatively simple cooling loop control system utilizing a single cooling coil in series with a thermistor controlled liquid nitrogen flow valve. One additional advantage of the Phoenix cooling system is the manually selected initial cool-down mode of operation which reroutes the venting GN_2 through the internal spectrometer housing, convectively aiding in the heat transfer process.

TABLE 1

SENSOR SPECIFICATIONS

Spectral Range (microns)	2 - 5.5
Throughput (cm^2-ster)	2×10^{-3}
Nominal Resolution (cm^{-1})	0.64
Retardation (cm)	1.56
Retardation Rate (cm/sec)	5
Sample Interval (microns)	0.95
Scan Rate (scans/sec)	2.9
Mono Frequency (kHz)	150
Sample Frequency (kHz)	50
Signal Frequency (kHz)	8.6 - 24
Interferogram Length at Sample Frequency (words)	16K
Throughput Match Wavelength (microns)	2.0
Detector:	InSb
Diameter (mm)	1.0
Temperature (°K)	77
Cryogen Hold Time (hours)	8
Cold Filter (removable)	CS 0-54 (Corning Glass)
Field of View: full angle (degrees)	35
Instrument:	
Temperature (°K)	250
Telescope Diameter (inches)	4
Field of View: full angle (degrees)	0.32
Beamsplitter: Coating	CaF_2:Si
Optical Elements	Ge
Obscuration with Secondary	0.14

Although the cooling system capability permits 220°K operation throughout the sensor, several components are maintained at elevated temperatures to insure reliable and accurate interferometer bearing operation. These components comprise the double cube interferometer assembly which is stabilized at 250°K by the use of contact heaters. In short, the sensor optical system is cooled to 220°K while the cube assembly is maintained at 250°K.

2.2.2 Spectrometer Description

The Phoenix sensor head contains: the main or "signal" interferometer and integral transducer assembly, the reference interferometer system, the detector/LN_2 dewar unit, the internal calibration source, and several key temperature monitoring and control devices.

Figures 2 and 3 contain a layout view of the Phoenix sensor.

Figure 2 reveals a heated door over the telescope entrance window which prevents abrasion of the window surface and accumulation of water or frost during instrument cooldown. In addition, the door contains a full aperture reference blackbody against which the instrumental background temperature can be measured for calibration purposes during operation at altitude.

The door mechanism is remotely actuated by a single planetary gear/DC motor assembly controlled via the flight control panel. The assembly drives a 30:1 reduction worm gear which provides the mechanical advantage necessary for positive sealing against moisture. In the event of power failure, the door is automatically closed via a fail-safe battery pack located in the control chassis.

To inhibit frost build-up on the external surface of the sensor top plate from interfering with instrument operation, a 400 Hz contact heater pad is mounted on the internal side of the top plate. The temperature of the top plate is controlled

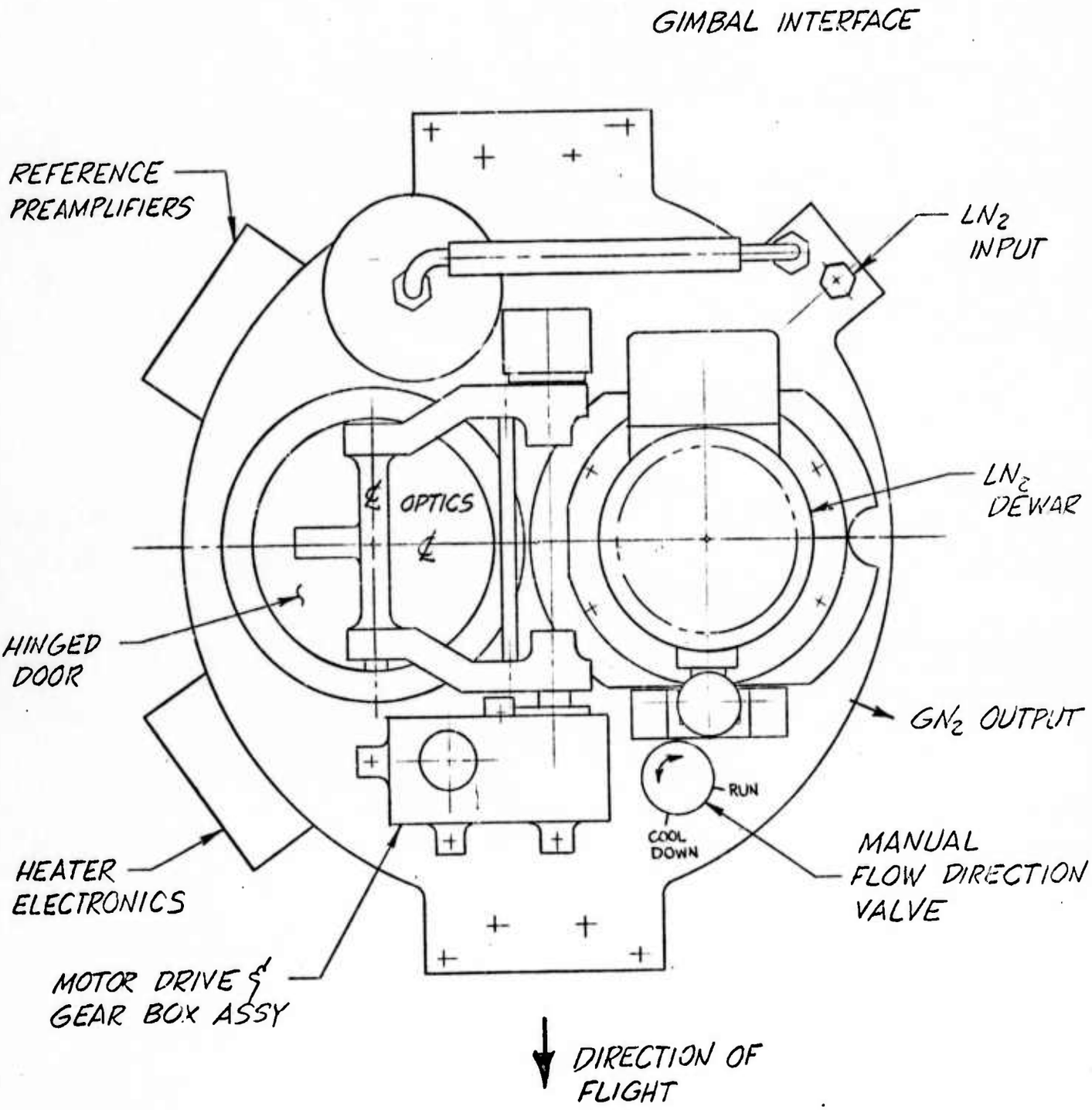

FIGURE 2

PHOENIX INSTRUMENT ASSY (TOP VIEW)

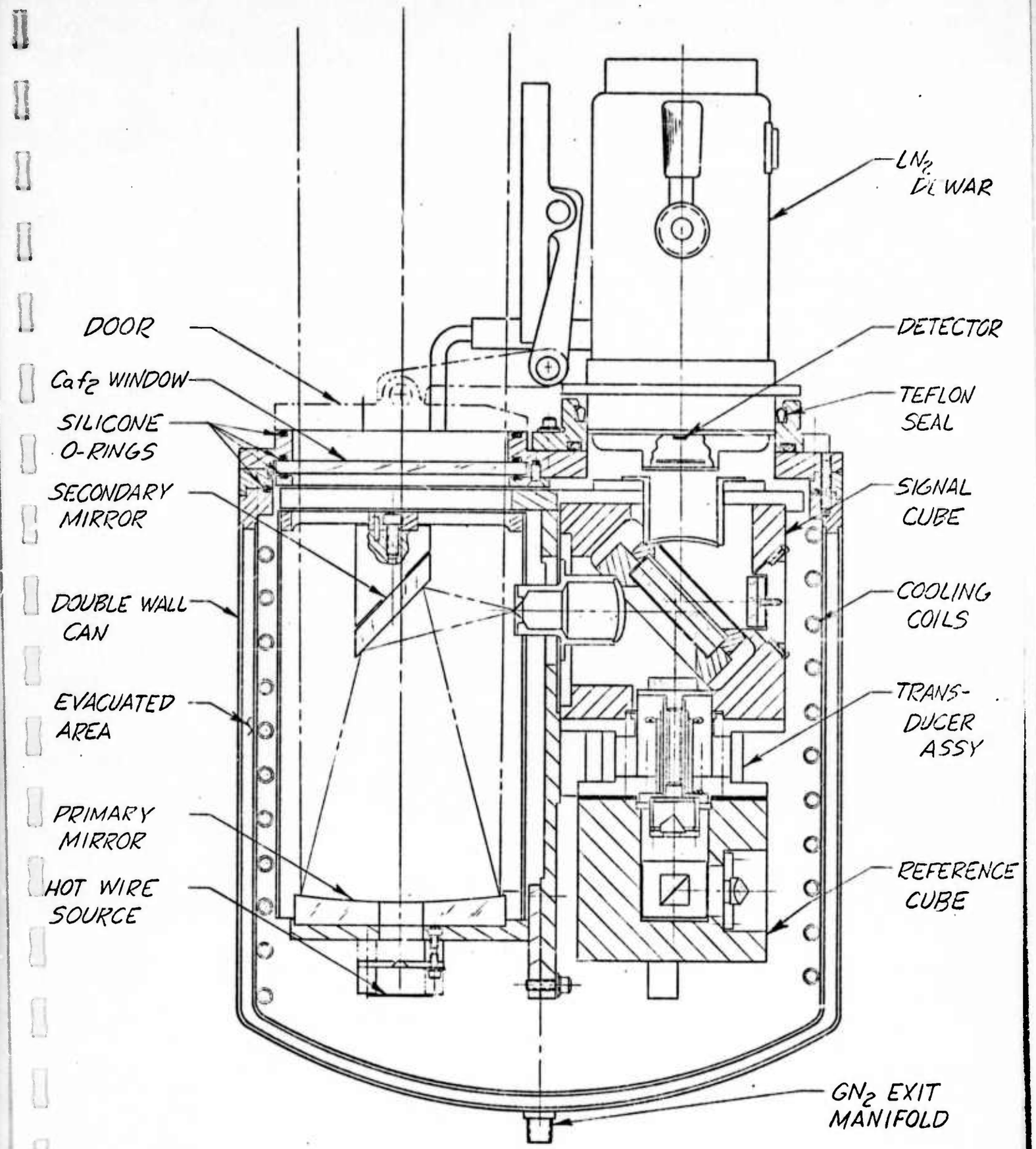

FIGURE 3

PHOENIX SPECTROMETER

to slightly above ambient temperature to insure minimum moisture condensation. The interferometer/telescope assembly which is supported via this top plate is thermally isolated from the warm section by phenolic standoffs.

The external instrument housing provides thermal isolation from ambient surroundings via a vacuum insulated double wall shell. This housing can be removed in its entirety, exposing the instrument for adjustment.

Figure 3 contains a layout view of the interferometer spectrometer including foreoptics. In this view, the reference laser is not shown, since it is mounted behind the reference cube assembly. Also not shown is the laser tube housing which completely encloses the laser minimizing thermal gradients.

The interferometers used in this instrument are of the conventional Michelson design, utilizing the phenomenon of interference to produce a spectrally encoded signature of the input energy referred to as an interferogram. The recovery of the spectral information is obtained by performing a Fourier transform on the resulting signal which may be thought of as a simple harmonic analysis of the interferogram.

The resolution $\Delta\nu$ (cm^{-1}) of a Michelson interferometer is inversely proportional to the optical retardation B (cm) of the spectrometer (i.e., twice the physical motion of the moving mirror) and is constant in wavenumbers throughout the spectrum. To achieve .64 cm^{-1} spectral resolution with the Phoenix sensor, a one-sided interferogram with a .78 cm maximum path difference between reflected and transmitted rays is required.

Spectral coverage to 5.5 microns is obtained by the use of germanium optics and a calcium fluoride beamsplitter, as well as a liquid nitrogen cooled indium antimonide detector. As mentioned previously, to enhance the sensitivity of the

spectrometer in the spectral region of interest, the sensor is cooled to temperatures approximating ambient temperatures at altitude. This cooled approach consists of a two level temperature control system utilizing liquid nitrogen supplied directly from the Firebird supply reservoir to cool the system optics to 220°K while 400 Hz heaters attached to the double cube assembly maintain the temperature sensitive interferometer bearing components at an elevated temperature of 250°K. The sensor cooling loop diagram is shown in Figure 4.

Accurate information concerning the position and velocity of the moving mirror is provided through the "reference" interferometer assembly. The designation "reference" comes about since the interferometer measures the instantaneous displacement of the moving mirror with respect to a reference position.

The reference interferometer for this particular instrument utilizes a double pass approach with corner cube retroreflectors inserted in place of the plane mirrors in a standard interferometer (Figure 5). The optical system doubles the optical retardation and hence doubles the frequency of the cosinusoidal signal from the monochromatic HeNe laser reference source. The effective wavelength of the source with this arrangement is .6328/2 microns. The advantage of using retroreflectors as the reflective elements in the reference interferometer is their insensitivity to tilt or wobble. This stability is of prime concern with the Phoenix optical head required to operate over a wide range of attitudes. In addition, for the desired wavelength coverage of 2 to 5.5 microns the minimum sampling interval required by the sampling theorem is one micron. The one micron sampling interval is easily synthesized from the optically doubled signal by taking

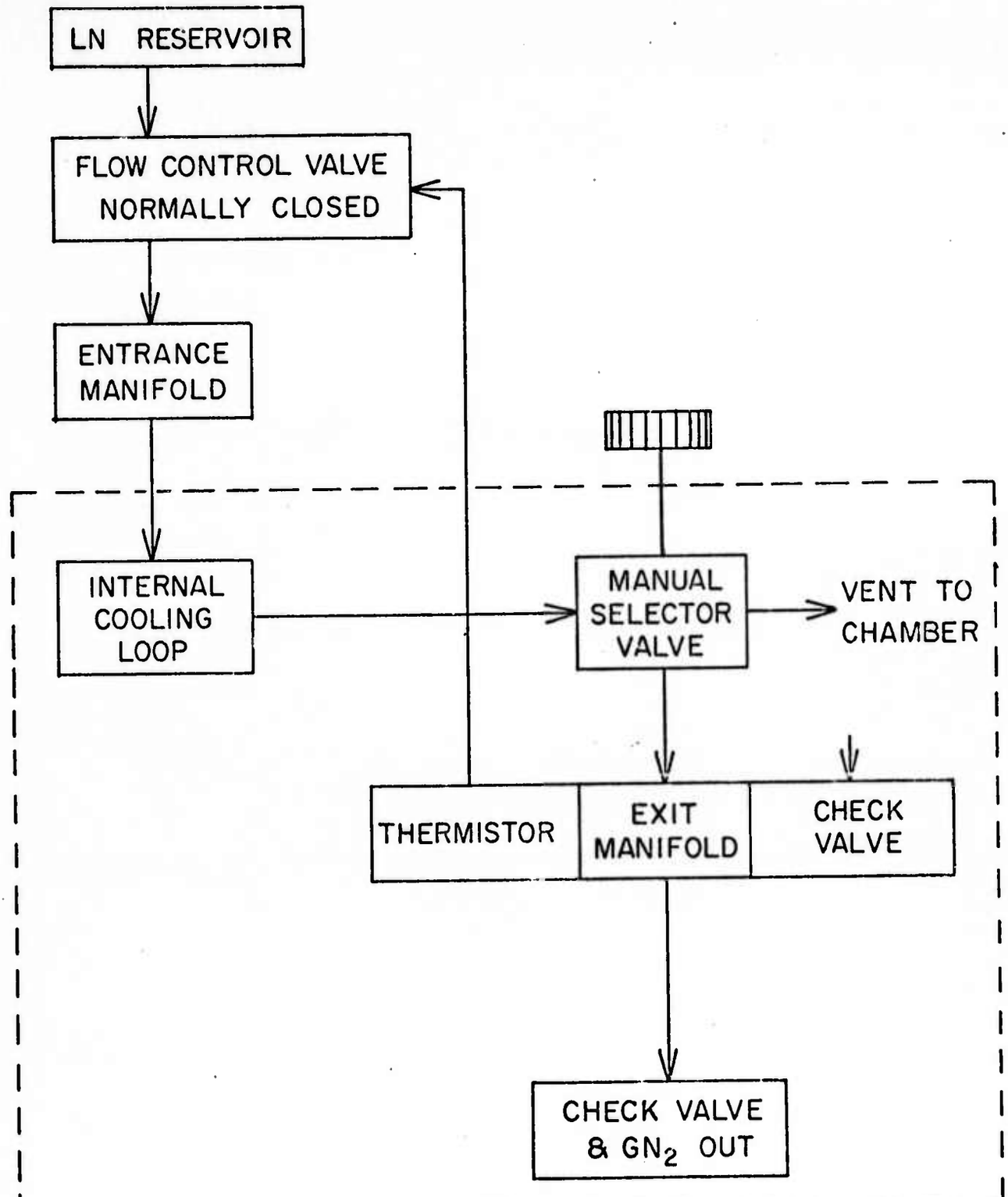

FIGURE 4

PHOENIX COOLING LOOP BLOCK DIAGRAM

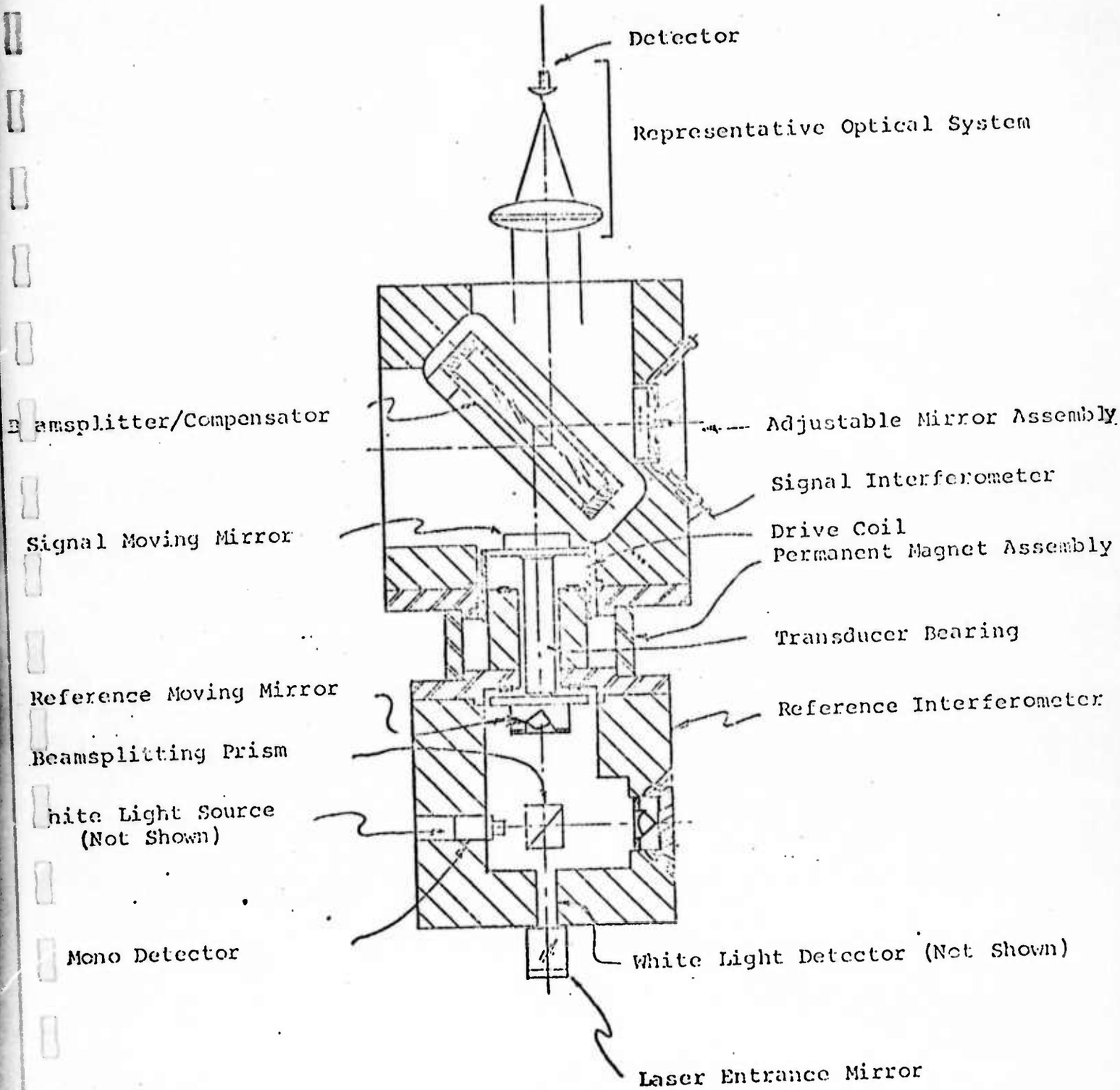

FIGURE 5

SIGNAL AND REFERENCE INTERFEROMETER

every third going positive zero crossing as the sample interval, the resulting sampling wavelength is (0.6328μ) x (3/2) or approximately 0.95 microns.

The actual scan length of the instrument is determined by the sampling interval - interferogram word count product which is obtained by binary counters which count the zero crossings in the monochromatic reference interferogram

$$B = (\lambda_s)\ (2^N)$$

where

B = optical retardation (cm)

λ_s = sampling wavelength (cm)

N = number of zero crossings, where 2^N = interferogram size

For the Phoenix sensor, the design constraints limited the interferogram word count to 16K (N = 14) points resulting in a retardation of 1.55 cm. The typical active scan rate of the sensor is 2.9 scans/sec based upon the retardation rate of 5.0 cm/sec with a 90% active duty cycle.

In addition to the monochromatic source, a white light reference generated by a tungsten lamp source and a germanium detector provides absolute positional information and serves as a starting point for the determination of scan length. The reference position or fiducial occurs at zero retardation, a unique position in the mirror scan where all energy is phase coherent. The white light interferogram is symmetric about this reference position with the peak interferogram amplitude proportional to the total energy modulated by the interferometer. The white light positional information serves the following purposes: first, it resets all the digital counters, enabling data collection to begin at the same position in the

scan with the required precision. Second, during retrace, it provides for reset termination and scan initiation.

The design of the bearing and transducer assembly which supports the moving mirror in the signal interferometer and the moving corner cube in the reference interferometer was the object of a considerable amount of effort during the design and development phase of the original Firebird program.

Essentially the bearing and transducer assembly consists of the two moving optical elements attached to an inner glass bearing. The assembly as a unit is located within a field generated by a permanent magnet. Scanning is thus accomplished by applying the proper voltage waveform to the coil causing the assembly to move in a manner similar to the voice coil moving in a loudspeaker assembly. This moving assembly is supported by a cylindrical outer bearing manufactured to tolerances such that the tilt of the bearing is held to within 10 arc seconds per centimeter of retardation (Figure 6). This tilt results in a weighted path length error across the aperture expressed as

$$\Delta\lambda_t = 0.424 \times \alpha \times B \times D$$

where

$\Delta\lambda_t$ = misalignment (cm)
α = tilt coefficient: 5×10^{-5} rad/cm
B = the optical retardation: 1.56 cm
D = the diameter of the mirror: 2.54 cm

Considering the shortest wavelength of interest for the Phoenix program to be $\lambda_s = 2.0$ μm, we can present the bearing tilt as a fractional part of λ_s using the above relation,

$$\frac{\Delta\lambda_t}{\lambda_s} < 0.42$$

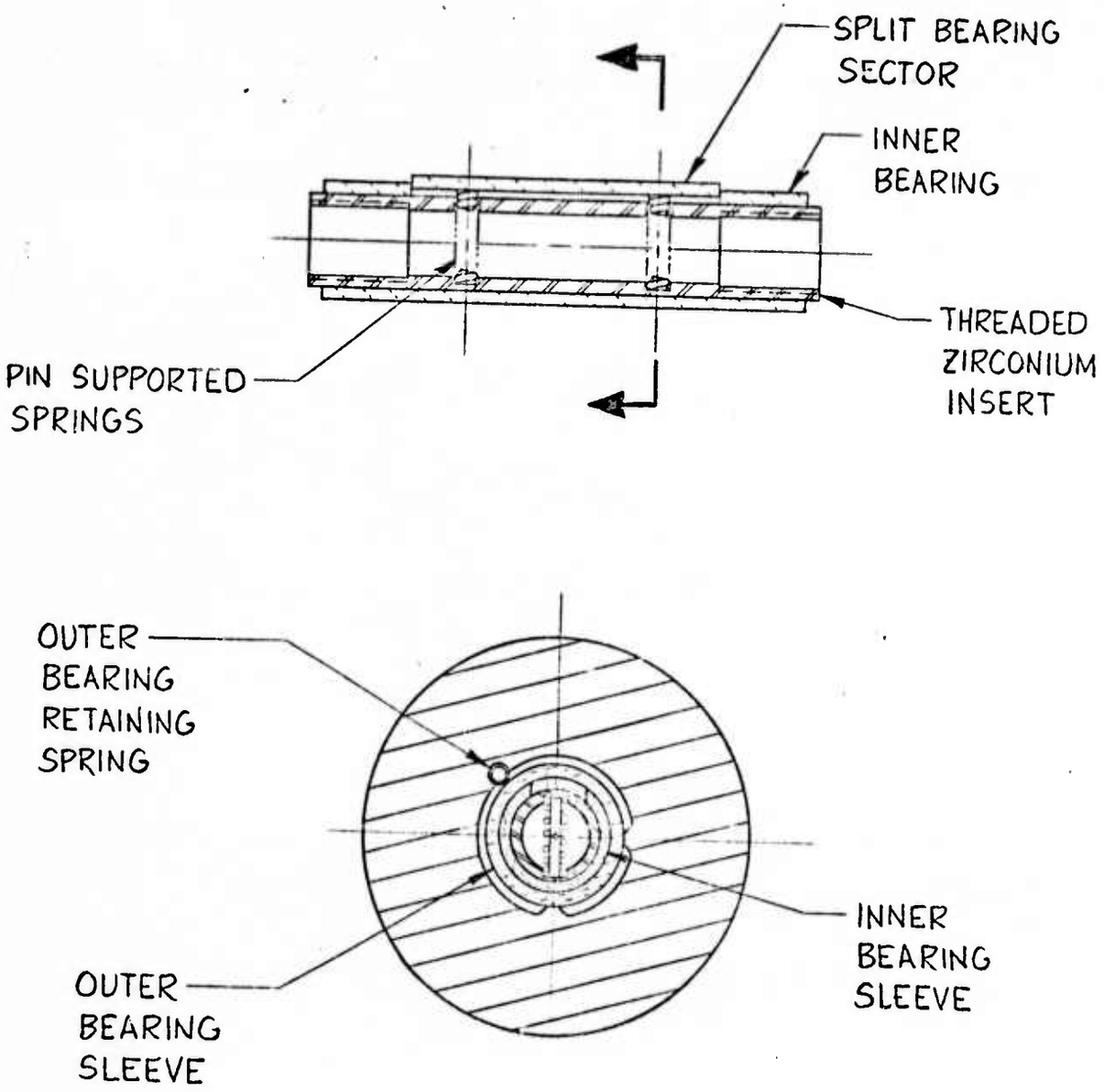

ASSEMBLED BEARING IN MAGNET POLE PIECE

FIGURE 6

BEARING ASSEMBLY

The effect of this tilt is to diminish the energy coherence at the end of the stroke, reducing resolution. The performance characteristics of the interferometer observed during the program acceptance test phase indicated that a measurable tilt factor, in excess of 10 arc seconds, currently exists in the bearing assembly. This observation is discussed further in Section 6.1.2.

As mentioned previously, the design of the signal interferometer incorporates an indium antimonide photovoltaic detector cooled to 77°K providing photon noise limited performance under reduced background conditions. This particular detector, a solid state device utilizing a diffused p-n junction, was manufactured by Barnes Engineering Company, Stamford, Connecticut. Parameters and characteristics of this detector as measured with a controlled background radiance are given in Table 2. The results indicate cooling the interferometer below ambient temperature does provide an improvement in sensitivity by a factor of 2.1. However, this increase in detectivity falls somewhat short of the improvement predicted strictly by photon flux reduction which is expressed as the following ratio

$$\left[\frac{Q_{0-5.5\mu\ (300°K)}}{Q_{0-5.5\mu\ (220°K)}}\right]^{1/2} = \left[\frac{2.2 \times 10^{14}}{6.3 \times 10^{12}}\right]^{1/2} = 5.9$$

This anomalous result is discussed further in Section VI describing the total system performance.

The final design for the Phoenix detector/dewar assembly includes provision for mounting an optional cold filter for 250°K sensor operation. This liquid nitrogen cooled glass filter reduces the spectral range of the sensor to 4.5 μm improving the sensitivity in the 2.0 - 4.5 micron region by further reducing the photon flux incident on the detector.

TABLE 2

INDIUM ANTIMONIDE DETECTOR

Detector	InSb, 77°K
Serial No.	614-74
Diameter, cm	0.10
Surface loss, η	0.68
Capacitance, pf	187
Dynamic impedance, MΩ	67(a)
Test Conditions	
Test frequency, Hz	1000
Noise bandwidth, Hz	50
Blackbody temperature, °K	500
300°K Background	
Detector F.O.V., full angle degrees	35
Photon flux, phot-sec^{-1}	2.2E + 14(b)
Flux density, watts-cm^{-1}	4.5E - 06
NEP_{pk}, watts-Hz$^{-1/2}$	5.2E - 13
Responsivity, amps-watt^{-1}	.441
$D^*(\lambda_{pk}, 1000, 1)$, cm-Hz$^{1/2}$-watt^{-1}	1.7E + 11
Reduced Background	
Detector F.O.V., full angle degrees	5
Photon flux, phot-sec^{-1}	6.3E + 12(b)(c)
Flux density, watts-cm^{-1}	4.5E - 06
NEP_{pk}, watts-Hz$^{-1/2}$	2.4E - 13
Responsivity, amps-watt^{-1}	.36
$D^*(\lambda_{pk}, 1000, 1)$, cm-Hz$^{1/2}$-watt^{-1}	3.63E + 11

(a) Measured viewing 77°K background

(b) Photon flux does not include surface loss

(c) Simulated 220°K background flux

The transmission curve for the filter, Corning CSO-54, is shcwn in Figure 7.

The expected sensitivity improvement with the filter in the system can be determined on the basis of the incident flux reduction. The actual filtered flux is calculated by integrating the filter transmission with the background flux to arrive at the incoming flux level at the detector surface

$$\Phi = [\int Q\ \eta_f\ \Delta\lambda] \quad x\ \frac{\theta}{\pi}$$

where

Φ = total photon flux entering detector, photons-sec^{-1}

Q = background photon flux density, photon-sec^{-1}-cm^{-2}-μm^{-1}

η_f = filter transmission, parameter at source-referred wavelength

$\Delta\lambda$ = spectral bandwidth, μm

θ = system throughput, cm^2-ster, 2.0×10^{-3} cm^2-ster

The flux calculated using this expression assumes background flux levels corresponding to a uniform instrument operating temperature of 250°K, consequently

$$\Phi = 8.7 \times 10^{10} \text{ photon-sec}^{-1}$$

Now, assuming the quantum efficiency is constant over the spectral range, and if the detector cutoff is included in the optical efficiency, the expression for the detector noise equivalent power, NEP, can be written

$$\text{NEP} = \frac{hc\nu}{\eta_s} \left[\frac{2\Phi\Delta f}{q_e}\right]^{\frac{1}{2}} \text{ watts-Hz}^{-\frac{1}{2}} \quad (hc\nu >> kT)$$

where

h = Planck's constant, 6.626×10^{-34} joule-sec^{-1}

c = velocity of light, 3.00×10^{10} cm-sec^{-1}

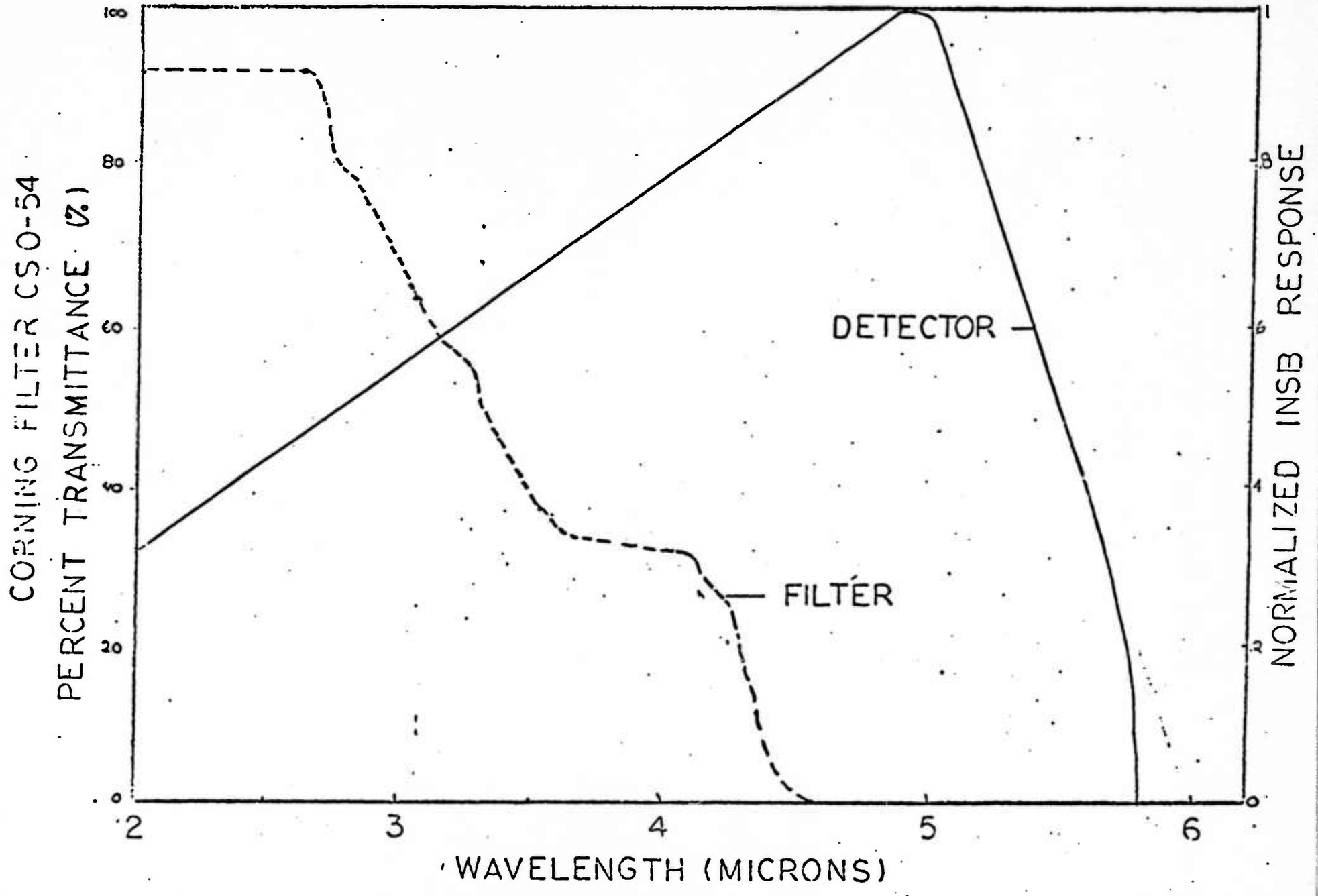

FIGURE 7

FILTER TRANSMISSION

ν = wavenumber, cm^{-1}

η_s = optical efficiency of detector and cold filter at source-referred wavelength

Φ = total photon flux entering detector, 8.7×10^{10} photons-sec^{-1}

Δf = electrical bandwidth, 1 Hz

q_e = detector quantum efficiency, 0.60

Thus for the wavelengths of interest

$$NEP(4.2\ \mu m, \text{filtered}) = 1.32 \times 10^{-13}\ \text{watts-Hz}^{-\frac{1}{2}}$$

$$NEP(2.7\ \mu m, \text{filtered}) = 6.03 \times 10^{-14}\ \text{watts-Hz}^{-\frac{1}{2}}$$

For a 250°K unfiltered background, the photon flux level can be determined from the following

$$Q_{tot} = 2.4 \times 10^{18}\ \text{photons-sec}^{-1}\text{-cm}^{-2}$$

$$Q_{0\text{-}5.5\mu m} = (1.6 \times 10^{-3}) \cdot Q_{tot}$$

or

$$Q_{0\text{-}5.5\mu m} = 3.9 \times 10^{15}\ \text{photons-sec}^{-1}\text{-cm}^{-2}$$

therefore

$$\Phi(250°K) = 3.0 \times 10^{13}\ \text{photons-sec}^{-1}$$

substituting into the expression for NEP results in

$$NEP(4.2\ \mu m, \text{unfiltered}) = 2.45 \times 10^{-12}\ \text{watts-Hz}^{-\frac{1}{2}}$$

$$NEP(2.7\ \mu m, \text{unfiltered}) = 1.12 \times 10^{-12}\ \text{watts-Hz}^{-\frac{1}{2}}$$

The improvement in sensitivity with the glass filter inserted can now be expressed as the following ratio

$$@\ 4.2\ \mu m \left[\frac{2.45 \times 10^{-12}\ \text{watts-Hz}^{-\frac{1}{2}}}{1.32 \times 10^{-13}\ \text{watts-Hz}^{-\frac{1}{2}}}\right] = 18.6$$

$$@\ 2.7\ \mu m \left[\frac{1.12 \times 10^{-12}\ \text{watts-Hz}^{-\frac{1}{2}}}{6.03 \times 10^{-14}\ \text{watts-Hz}^{-\frac{1}{2}}}\right] = 18.6$$

In practice, the detector experiences the lower flux levels consistent with a 220°K background with the interferometer operating at 250°K resulting in a slight increase in the improvement factor calculated above.

2.2.3 Optical Design

The optical layout of the Phoenix spectrometer is shown in Figure 8 (see Table 3 for description). The optical system is comprised of a cooled Newtonian telescope assembly, entrance field stop, and the interferometer.

Energy enters the spectrometer through the cold calcium fluoride window and is focussed at the entrance field stop by the telescope optics. The energy is then collimated by the interferometer entrance lens into the interferometer signal cube, and is finally focussed by the exit lens onto the detector. The field of view of the instrument is 5.6 mrad full angle.

2.2.4 Cryosystem

The Phoenix cryosystem consists of the Firebird LN_2 storage reservoir, including vacuum insulated transfer line, and the sensor head cooling loop. The system cooling loop block diagram is shown in Figure 4.

Pressurized liquid nitrogen is supplied to the optical head via the LN_2 storage tank, transfer line, and flow control

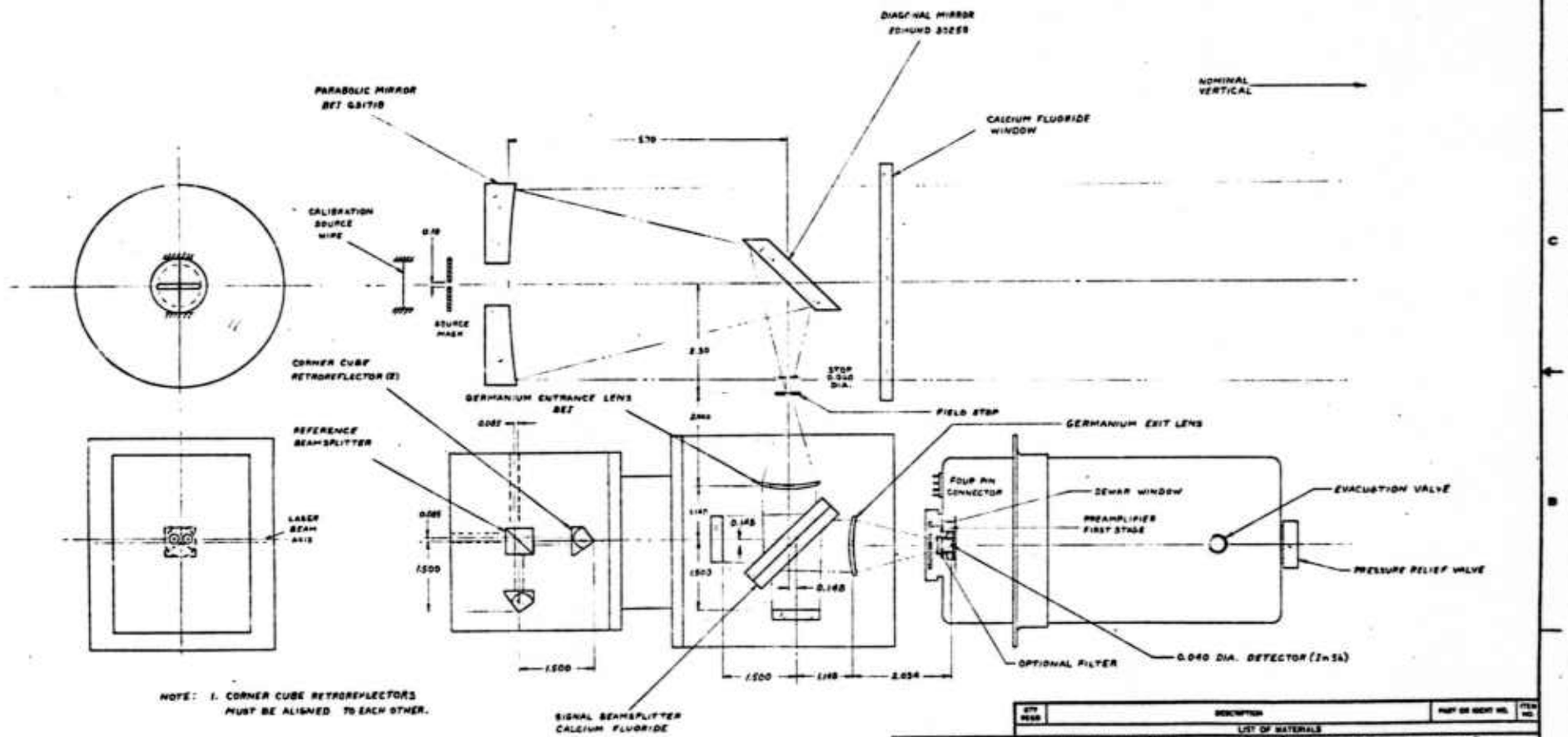

FIGURE 8

OPTICAL LAYOUT

Block Engineering, Inc.
CAMBRIDGE, MASSACHUSETTS

PHOENIX
OPTICAL DIAGRAM

D | 21351 | 641345

Element	Surface Number	Radius of Curvature	Clear Aperture Diameter	Distance to Next Surface	Material	Appropriate BEI Dwg.
Window	1,2	Infinite	4.250	8.000	CaF_2	623327
Paraboloidal	3	8.5	4.00	5.70	Fused Silica	632166
Secondary	4	Infinite	1.500x2.120	2.30	Pyrex	Edmund 30258
Entrance Field Stop	5	Infinite	.060	2.00	Aluminum	623375
Entrance Lens	6,7	2.004 2.847	1.130	1.148	Germanium	623396
Beamsplitter/ Compensator	8	Infinite	2.000	1.500	CaF_2	631581
Fixed/Moving Mirror	9	Infinite	1.000	1.500	Quartz	623351
Beamsplitter/ Compensator	10	Infinite	2.000	1.148	CaF_2	631581
Exit Lens	11,12	1.985 2.781	1.130	1.634	Germanium	623397
Dewar Window	13,14	Infinite	-	-	Corning glass	641340
Cold Filter (Optional)	15,16	Infinite	0.400	0.250	Corning glass	623309
Detector	17	Infinite	.039	-	InSb	8001230-0
Reference Beamsplitter	-	-	.600 x .300	-	BK-7	623324
Corner Cube Retroreflectors	-	-	.500	1.500	BK-7	623320
Calibration Source Mask	-	-	.010 x .090	-	Aluminum	623376

(dimensions in inches)

TABLE 3

OPTICAL SYSTEM PARAMETERS

(see Figure 8)

valve. Originally, the cryosystem included a liquid nitrogen gas generator which accepted the liquid nitrogen from the reservoir and generated cold gaseous nitrogen which was circulated at variable rates through the sensor cooling coils. Unfortunatley, the unreliability of the unit (see Section V) resulted in a modification to the cryosystem to allow direct transfer of liquid nitrogen to the sensor head. The liquid nitrogen delivered to the sensor is circulated through a single cooling coil mechanically attached to the double wall instrument housing, providing radiative and conductive cooling of all internal components. Typically, this heat transfer process raises the temperature of the nitrogen to approximately 220°K, generating cold gaseous nitrogen within the coil. During normal operation this gas is vented directly to ambient via a 4 psig check value. However, during initial sensor cooldown this cold gas is used to convectively enhance the thermal transfer by venting the GN_2 directly intc the instrument chamber. Venting the gas through the instrument allows it to take up a considerably larger amount of heat during cooldown, while the coil is sufficient by itself during cold operation. This technique allows the sensor to cool fairly rapidly, requiring 200 moles of gas or 7 liters of liquid nitrogen to cool the system in approximately 2 hours.

The control loop associated with the cooling system utilizes a calibrated thermistor attached to the cooling loop exit manifold. As the temperature of the exit gas varies, the voltage across the thermistor varies accordingly. The resultant voltage is referred to the input of the flow control valve driver circuit located in the electronics chassis. The circuit has a preset threshold hysteresis which corresponds to an 8°K temperature differential between valve mode changes, e.g., 227°K valve opens, 219°K valve closes. The valve

hysteresis optimizes the cooling loop duty cycle to approximately 50% at altitude insuring in excess of 4 hours cooling capacity.

2.2.5 Interferometer Electronics

The interferometer head electronics consist of the signal detector and preamplifier, the reference detectors and preamplifiers, the laser and DC-DC converter supply, the piezoelectric mirror adjust, and the transducer drive coil (see Figure 9).

The indium antimonide detector operating over 2 - 5.5 microns produces spectrally encoded signals in the 8.6 - 24 kHz region requiring a preamplifier with extremely low noise characteristics over a wide range of frequencies. The preamplifier designed for this system incorporates a dual FET input stage coupled to a standard operational amplifier circuit whose gain has been optimized for this particular detector. The noise contribution of the preamplifier, less than 2 nanovolts per root cycle input noise voltage, is such that the photon generated noise of the detector is the limiting noise in determining the sensitivity of the instrument. The signal output from the preamplifier passes through the signal cable to the Phoenix signal card located in the control electronics chassis.

The reference detectors, silicon (HeNe), and germanium (white light) are located at the exit of the reference cube and are the source of information regarding transducer velocity and position.

The reference preamplifiers consist of an FET buffer and a high gain-wide bandwidth operational amplifier with high current ouput capability designed to decrease the ouput impedance of the lines carrying the signal to the control chassis while

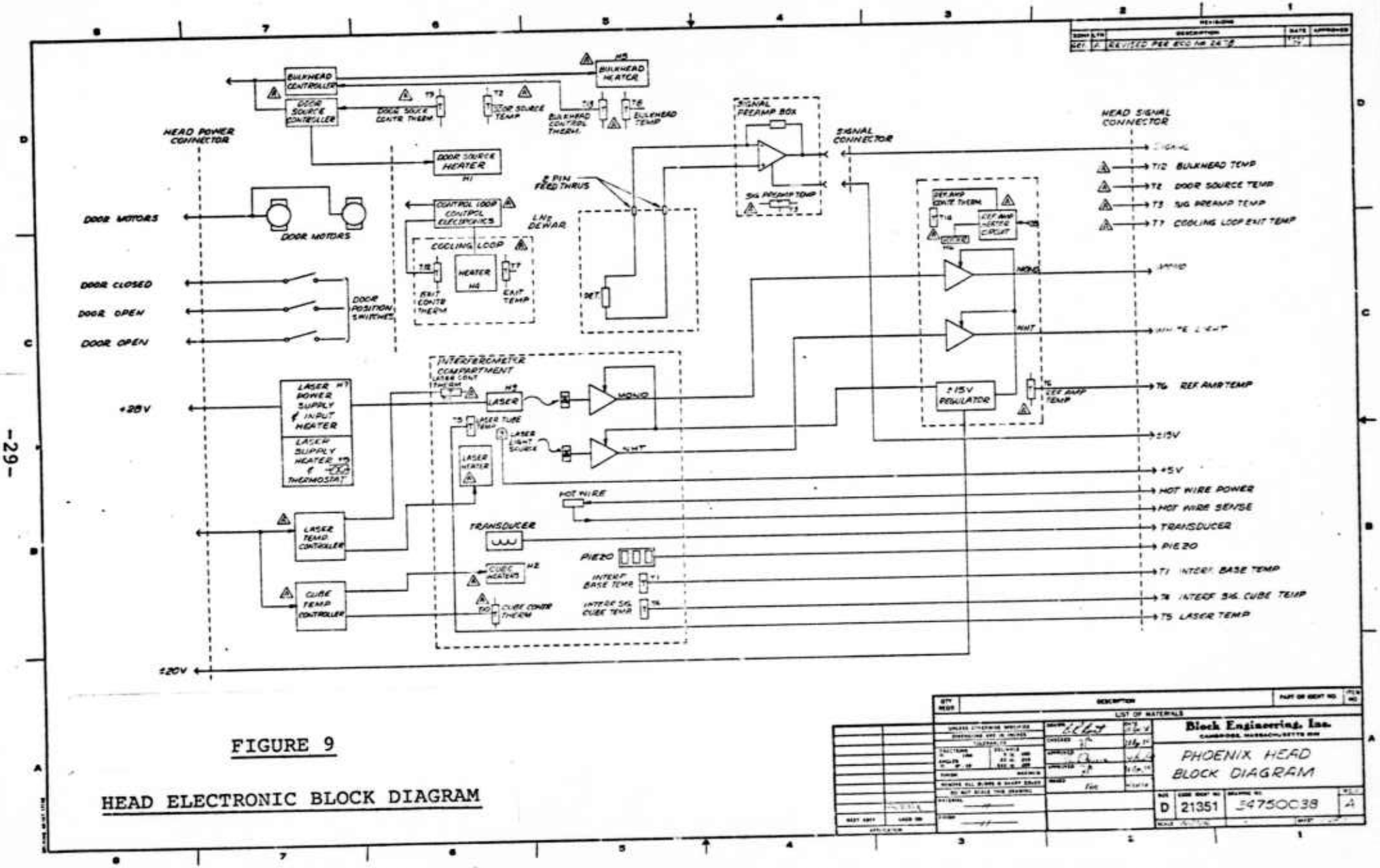

FIGURE 9

HEAD ELECTRONIC BLOCK DIAGRAM

Block Engineering, Inc.
CAMBRIDGE, MASSACHUSETTS

PHOENIX HEAD
BLOCK DIAGRAM

SIZE D | CODE IDENT NO. 21351 | DRAWING NO. 34750038 | REV A

introducing some gain to the reference signals. The preamplifiers are located in the aft junction box.

The laser DC-DC converter provides a 1.5 KV-DC filtered bias to the HeNe laser during normal operation. The supply is externally mounted on the door motor drive housing and is qualified for low temperature-low pressure operation. Primary power to the converter is an unregulated 28V-DC is supplied by the aircraft.

The piezoelectric fixed mirror adjust operates on a ±400 V-DC supply. Variations in the DC level result in a corresponding variation in the fixed mirror alignment in the signal interferometer via piezoelectric elements attached to the mirror mount. The two elements are arranged to provide for a tilt of the fixed mirror about two orthogonal axes. The alignment controls are located on the flight control panel.

Elevated temperature control of the interferometer, the top plate, and the door source is maintained via three independent servo control loops. Each temperature controller consists of a simple servo loop comprised of a thermistor bridge circuit, zero crossing AC Trigac, time proportioning circuit, Triac, and heater blankets. The significant features of the temperature controllers are small size, less than one half percent error from set point, high efficiency power transfer, and negligible radiated power. Separate thermistor readouts are provided for GSE panel monitoring of the component temperatures.

The ancillary electronics consist of the telescope door electronics and the hot wire calibration source.

The door assembly is controlled via the system command panel. Activation of the switch energizes a relay which engages the 28V-DC motor. The door travel is limited by contact switches in the closed and retracted positions.

The hot wire calibration source provides the internal signal during the pre-flight checkout. The source consists of

a 1.5 Ω Nichrome wire which is heated by a direct current. The voltage across the wire is closely regulated via a bridge circuit so that the resistance is held constant, consequently, the radiance will be stable with time.

2.2.6 Control Electronics

The measurement system electronics control the operation of the interferometer, LN_2 storage vessel, and the telescope door mechanism as well as the tape recorder and gimbal mount. The circuitry is arranged on printed circuit cards according to related control functions. The interchange of sensor heads requires a similar interchange of all plug-in PC cards with cards specifically designed to provide unique control of the Phoenix sensor. Functionally, a majority of the Phoenix circuitry is identical to the Firebird electronics, allowing card for card replacement without hardware modifications to the system wiring.

SECTION III

PROCUREMENT

3.0 General

Since virtually all of the components used in the fabrication of the Phoenix system were purchased from outside vendors, a major portion of the early program effort was involved with procurement. This effort required and received the close cooperation and coordination of the Engineering, Quality Assurance and Reliability, and Purchasing departments. Purchase specifications were written, vendor capabilities were evaluated and vendor surveys run, all received parts and material were 100% inspected and/or tested to assure conformance to the specification and purchase order requirements.

SECTION IV

SYSTEM DEVELOPMENT/QUALIFICATION

4.0 General

The successful completion of the Phoenix program was contingent on the development and qualification of interferometer components insensitive to low temperatures and varying attitudes. Much of the early developmental work centered on the interferometer bearing qualification for low temperature operation. This initial work was a direct extension of the primary develpomental effort of the Firebird program to design, construct, and successfully test a cryogenic interferometer bearing capable of precise linear motion over the entire sensor tracking range; ± 30° pitch, ± 10° roll from zenith. The end result of this multiprogram effort is discussed in the following section with particular emphasis on the Phoenix application. In addition to the bearing discussion, the section also includes a brief description of the low temperature qualification of various other sensor components as well.

4.1 Component Qualification

The sensor components assembled and tested for low temperature operation included: the reference interferometer, the signal interferometer, the HeNe reference laser, and the numerous vacuum seals associated with the interferometer and external can.

Initially, the interferometer cubes were tested under static conditions. The test configuration consisted of a "cold chamber" with transparent panels for viewing shifts in the fringe pattern produced by the two stationary interferometer reflecting elements illuminated with a monochromatic helium

line source. Both the signal and reference cubes maintained alignment to within 10 visible fringes at 80°K, well below the operating temperature range of the Phoenix sensor.

The second phase of the interferometer qualification was the verification of the sensor characteristics under dynamic conditions. The test arrangement consisted of a reference interferometer, signal interferometer, and spring loaded bearing assembly. A hot wire source was positioned in front of the signal cube entrance lens providing a controlled source of energy to monitor. The detector used with this configuration was a standard PbSe room temperature detector.

The instrument was successfully operated in the vertical mode, the actual sensor orientation, exhibiting excellent running characteristics at the specified operating temperature of 250°K. Following additional iterative testing employing low temperature piezoelectric compensation, the sensor was successfully operated at 220°K. During each low temperature test of the instrument, the tilt characteristics of the sensor in various operating altitudes were monitored by observation of the peak to peak interferogram signal (see Figure 10). In the final configuration, the amplitude stability of the signal was within 10% of the peak signal measured in the vertical position for all required attitudes.

During low temperature operation of the sensor, it was observed that the HeNe reference laser, Hughes Model 3121 H-P, would detune severly if temperature gradients, in excess of 30°K, were supported along the tube length. A failure analysis indicated the problem was due to the unique construction of the laser cavity which utilizes an integral plasma tube-resonant

Date: 28 May 1974
Test No: 28
Temp: 250°K

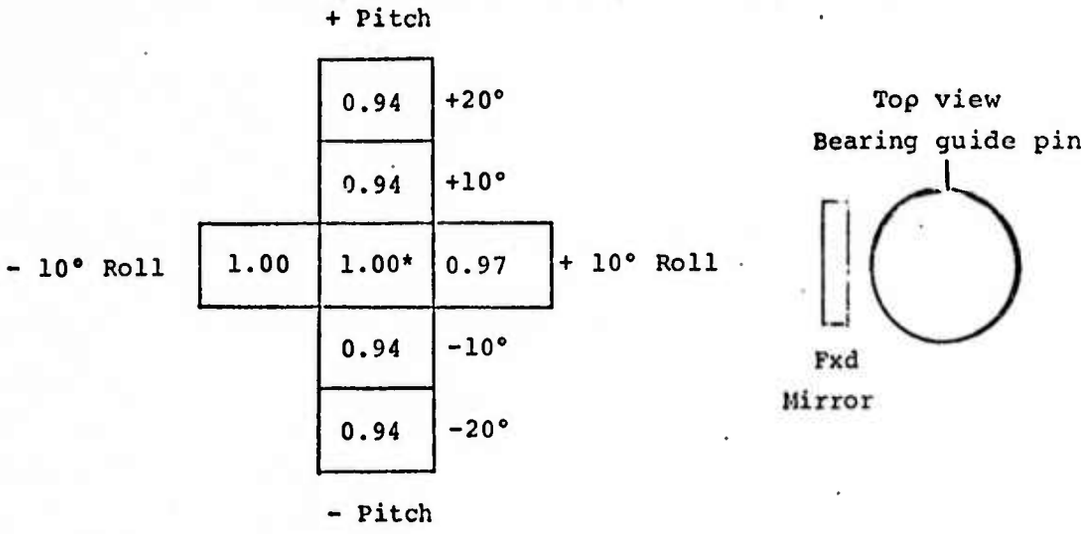

* Normalized peak to peak interferogram amplitude with bearing vertical.

Date: 25 June 1974
Test No: 31
Temp: 220°K

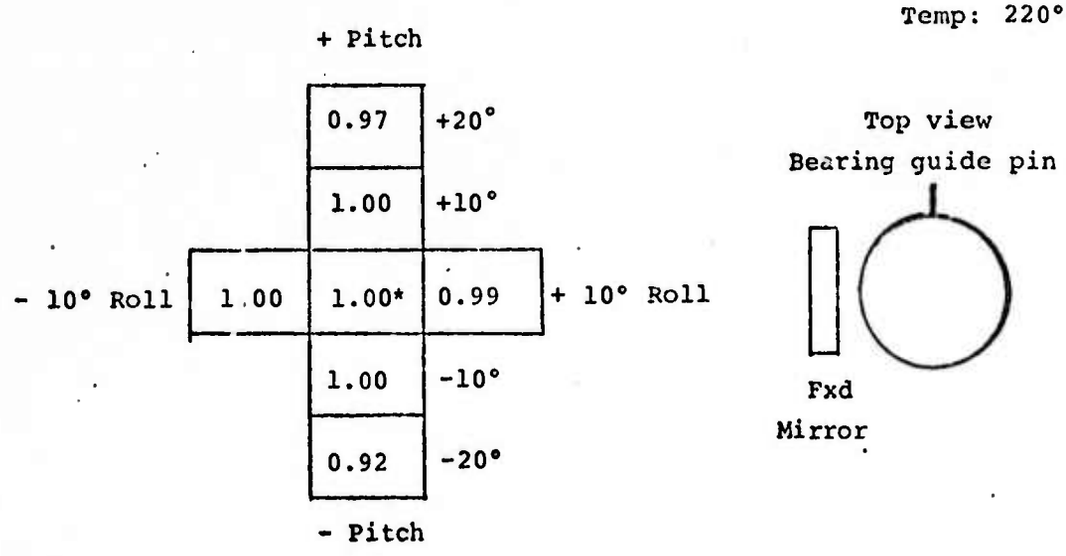

* Normalized peak to peak interferogram amplitude with bearing vertical

FIGURE 10

TILT SENSITIVITY

cavity assembly. The cavity mirrors for this unit are held in place with an epoxy based cement suitable for stable uniform temperature operation. However, the thermal properties of the epoxy are such that a relatively small variation in temperature along the tube length produced a significant stress on the epoxy held components resulting in cavity misalignment. The vendor was appraised of the problem and subsequently furnished a modified version of the integral cavity laser employing glass to glass seals which were qualified for dynamic as well as low temperature operation. The availability of this modified laser is not expected to present a problem in itself as the revisions have been incorporated into the vendor's standard unit. In addition to the modified laser construction, convective currents circulating around the laser are minimized with the design of a laser enclosure utilizing superinsulation to maintain a uniform temperature in a semistatic environment.

The qualification of various vacuum seals for low temperature operation consisted of a complete evaluation of metal "C" rings, spring loaded teflon seals, and silicone "O" rings in test setups closely approximating the actual sensor configuration. Each seal was chosen for evaluation based upon the material thermal characteristics and seal resiliency as well as cost and availability. The results of the repeated low temperature high vacuum cycling of each component indicated vacuum rated performance of properly prepared silicone and teflon seals to temperatures approaching 190°K while the effective range of the metal seals was found to extend to liquid nitrogen temperatures. The decision to use silicone and teflon seals throughout the sensor was based primarily on their cost and fieldworthy construction.

4.2 Interferometer Bearing Development

One of the primary objectives of the program development phase was the qualification of a low temperature bearing mechanism providing the highly precise motion of the moving mirror required in all tracking attitudes. Previous work with cryogenic bearing mechanisms undertaken during the Firebird program resulted in the design and construction of a unique interferometer bearing assembly incorporating a constant spring pressure to insure minimum tilt or wobble of the moving bearing over the entire stroke. Unfortunately, the development and qualification of this bearing expended a significant portion of the Firebird program time and funds without a substantial return in working hardware resulting in an extension of the low temperature qualification effort to the Phoenix program. Essentially, the Phoenix effort entailed repeated low temperature cycling of an assembled sensor, observing bearing dynamic characteristics with the sensor orientated in various operating attitudes, making appropriate modifications as necessary.

The bearing developed for the Firebird/Phoenix programs after considerable time and effort consists of a spring loaded glass inner bearing with a threaded zirconium mirror mount epoxied to each end, a spring loaded glass outer bearing sleeve, and a dry film lubricant (see Figure 11). The outer glass bearing sleeve contacts the surrounding magnet assembly at two orthogonal points with a coil spring providing a force of 250 grams under a 1 g environment, five times the mass of the moving assembly, at a third contact point. As the surrounding magnet iron contracts due to low temperature, essentially all of the force is transferred to the spring rather than the bearing sleeve, resulting in a constant external compression on the sleeve independent of temperature.

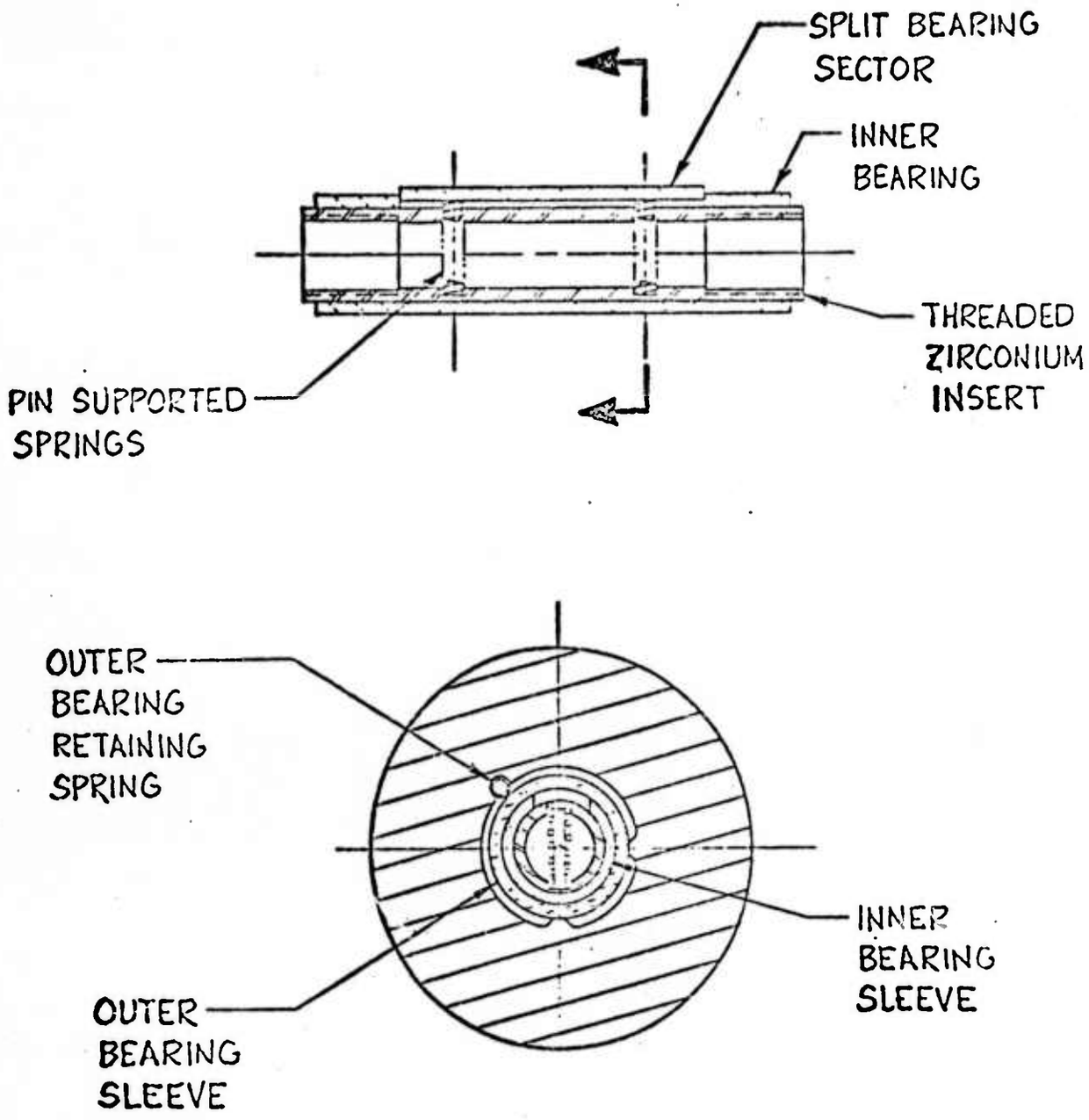

FIGURE 11

ASSEMBLED BEARING IN MAGNET POLE PIECE

(2) Orientation stability: signal interferogram stability shall be within 10% of the measured peak at a vertical position for all tracking altitudes, pitch ± 30°, roll ± 10°.

(3) Rotational bearing tilt: less than 0.5 arc minutes per 180° rotation.

(4) Longitudinal bearing tilt: less than 10 arc seconds per centimeter stroke.

(5) External stress components on the outer fixed bearing shall be a uniform minimum.

Initial qualification of the bearing for low temperature operation consisted of visual inspection of the static alignment in "cold chamber" tests. Typically, the shift at 220°K was less than 15 fringes in the visible corresponding to a mechanical motion of 6 arc seconds over the entire bearing length. As a second check, the bearing tilt was measured using autocollimation techniques at room temperature. The results were in good agreement with the cold chamber observations indicating stable low temperature dynamic operation was possible. Autocollimation techniques were also used to measure the rotational runout of the bearing under static room temperature conditions. The rotational tilt was measured at 0.5 arc minutes per 180° rotation, considerably better than previous cryogenic bearing designs.

The second phase of the bearing qualification consisted of dynamic operation with a complete interferometer assembly, monitoring the transducer drive voltage waveform and the peak to peak signal interferogram for shifts in the operating characteristics of the bearing, see Table 4 for a typical dynamic operation data sheet. Excellent running characteristics were obtained during this dynamic testing phase. The transducer

TABLE 4

INTERFEROMETER DRIVE DATA SHEET

1.0	Instrument	Phoenix	Serial No.
1.1	Retardation	1.56 cm	Cube Temp. 251.8 °K
1.2	Date	20 May 1974	Time 1610
1.3	Transducer Attitude	Vertical	
2.0	Reverse Direction Pulse Time	6.0	ms
2.1	Reverse Direction Pulse Amplitude	+17	volts
2.2	Reverse Direction Time	80	ms
2.3	Reverse Direction Amplitude	+7.8	volts
2.4	Reverse Mono Frequency	280	KHz
2.5	Reverse Mono Amplitude	9.0	Vpp
2.6	Reverse WHT Light Amplitude	27	Vpp
3.0	Stop Start Pulse Time	0.8	ms
3.1	Stop Start Pulse Amplitude	-7.5	volts
4.0	Forward Scan Time	250	ms
4.1	Forward Scan Voltage	-2.0	volts
4.2	Forward (Mono) Stop Time	0.25	ms
4.3	Forward Mono Frequency	100	KHz
4.4	Forward Mono Amplitude	9.0	Vpp
4.5	Forward WHT Light Amplitude	27	Vpp
5.0	Position Error Amplitude	+ 3.5 + 0 + 4.5	volts
5.1	Velocity Error Amplitude (Middle of Scan)	20m	Vpp
5.2	Velocity Error Amplitude (At Beginning of Sync)	+1.0	Vpp
5.3	Time Between Forward and Reverse WHT Light	2	ms
5.4	Reverse Stop Time (Time Taken to Stop in Reverse Direction)	0.7	ms
6.0	Position Summing Resistor	5.6K||11K	R45
6.1	Velocity Summing Resistor	5.6K||11K	R20
6.2	Position Integrating Capacitor	0.047	C14
6.3	Position Input Resistor	15K	R43
6.4	Start Stop Pulse Capacitor	0.33||0.22	C13
6.5	Reverse Direction Pulse Capacitor	2 µf	C11
6.6	Reverse Direction Amplitude Resistor	3.6K||9K||5.1K||10K	R24

servo loop parameters required only slight adjustment to compensate for the slightly stiffer motion of the bearing at 250°K. In addition, the tilt sensitivity of the instrument at this temperature was virtually nonexistent with the peak to peak signal interferogram varying less than 10% in all tracking attitudes. This observation generally substantiates the accuracy of the static testing performed on the bearing assembly.

Dynamic operation of the sensor at 220°K was accomplished at the close of the testing phase. The sensor performed successfully using the same qualification criteria as above with only minor servo loop adjustments. The orientation stability of the sensor at 220°K was in good agreement with the 250°K data (see Figure 12).

The decision to maintain the double cube assembly, including the bearing mechanism, at 250°K had been made prior to the successful operation of the sensor at 220°K. This commitment was based primarily on the extensive test data compiled indicating the stable reliable performance of the sensor operating at 250°K. Additional iterative testing of the sensor at 220°K would be necessary to qualify the instrument in such a manner.

Date: 24 June 1974
Test No: 30
Temp: 250°K

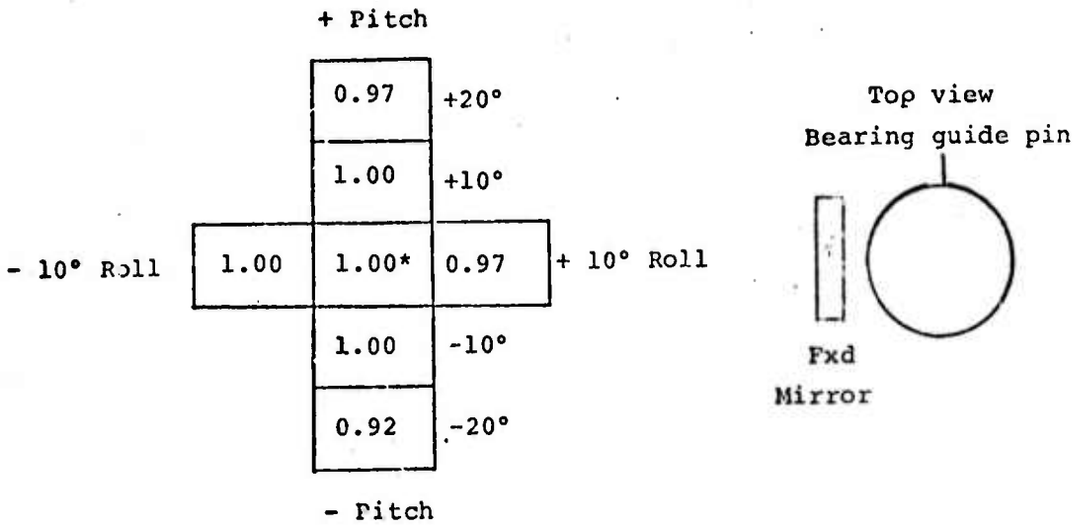

* Normalized peak to peak interferogram amplitude with bearing vertical.

Date: 25 June 1974
Test No: 31
Temp: 220°K

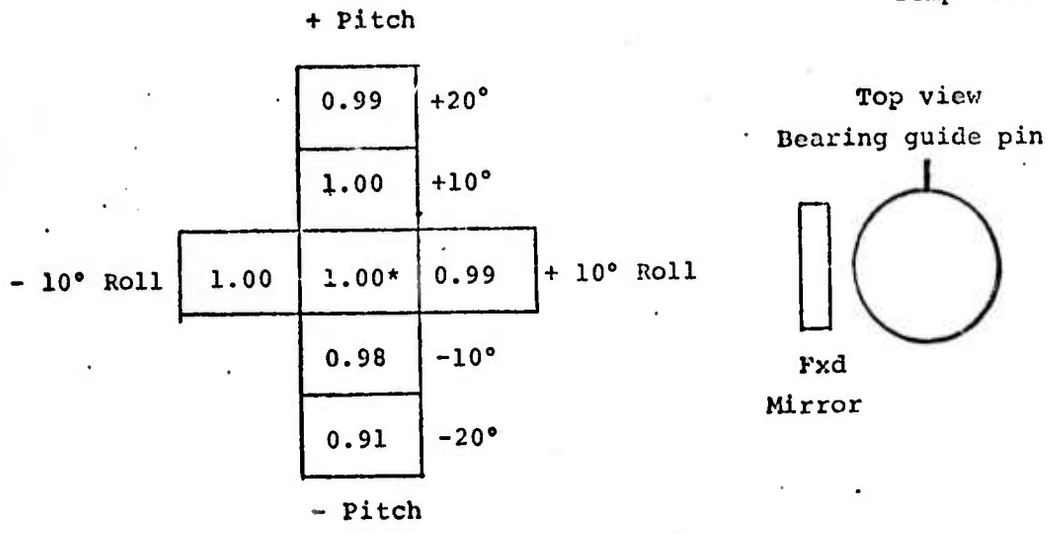

* Normalized peak to peak interferogram amplitude with bearing vertical

FIGURE 12

ORIENTATION SENSITIVITY AT 220°K

SECTION V

SENSOR CONSTRUCTION AND OPERATION

5.0 General

A fully functional interferometer spectrometer head was constructed at Block Engineering, Inc., Cambridge, Massachusetts and completed for final acceptance testing in October 1974. The assembled sensor (Figure 13) was integrated with the Firebird system and operational tests were performed at the contractor's facilities demonstrating the full system capability. Actual operation of the system is covered at length in the various subsystem operating and maintenance manuals and drawings, schematics and informational material which have been supplied to the user organization.

The following listing describes the problems encountered during the manufacturing and test operation phase and describes the analysis and subsequent corrective action taken in each instance.

5.1 Major Problems and Corrective Action

Component Failures

A. Liquid Nitrogen Gas Generator, Cryogenic Associates, Inc. Block Engineering Drawing No. 632181-A

Description of Problem:

(1) Internal heater failure

(2) Large electrical leakage path between liquid level sense elements and housing, degrading level sense dynamic range

Failure Analysis and Corrective Action:

(1) Heater failure mechanism identified as water condensation in the heater element during vendor assembly

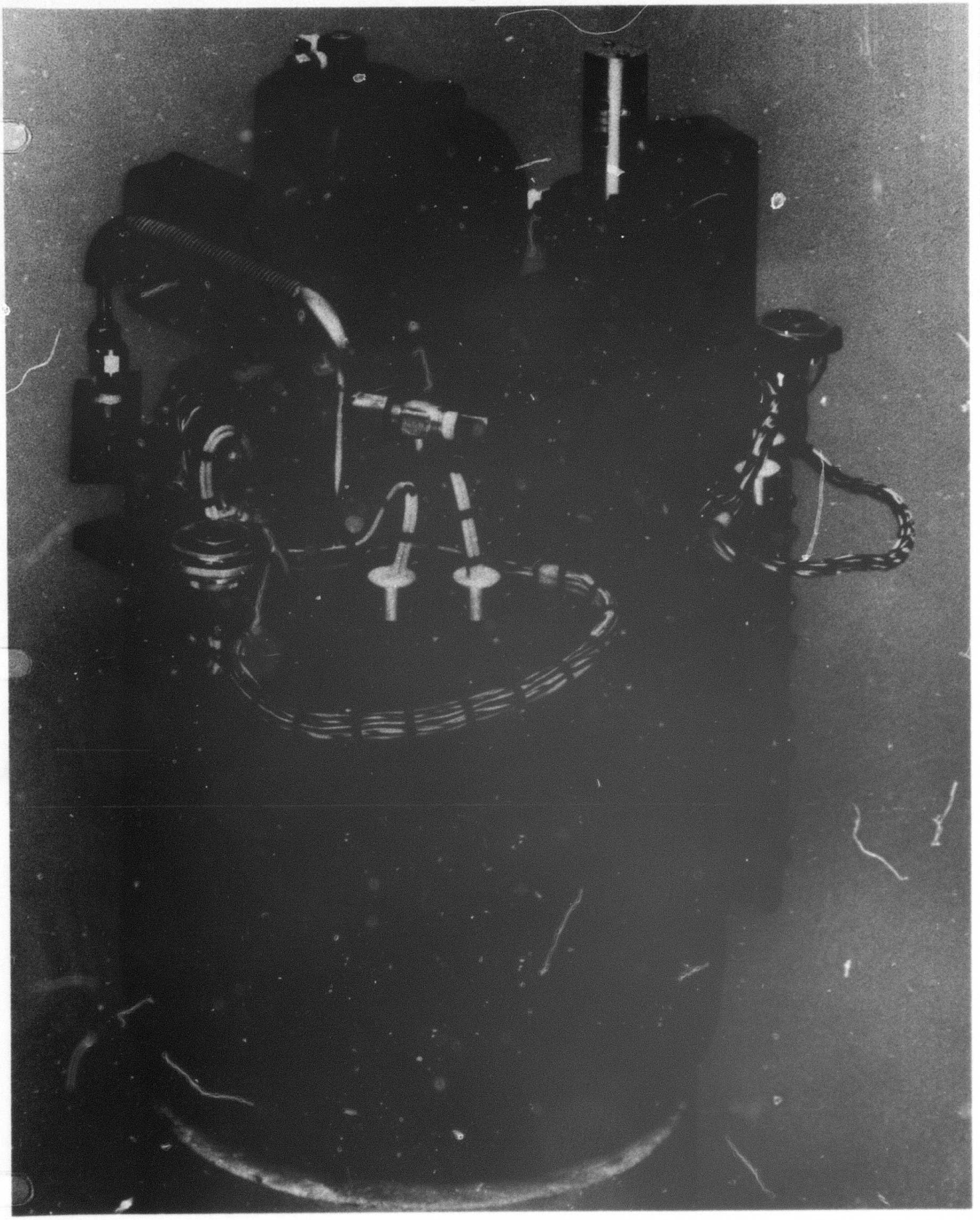

FIGURE 13

PHOENIX SENSOR

(2) High leakage to casing attributed to the multiple layers of superinsulation surrounding the electrical heater and level sense leads providing a shunt capacitance to ground

(3) Unit returned to vendor for refurbishment

(4) Subsequent testing of the modified gas generator produced a second heating element failure due once again to excess moisture condensation. The decision was made at this point to eliminate the gas generator in favor of a direct liquid nitrogen transfer path from the LN_2 storage reservoir to the sensor cooling loop. Functionally, this new approach was essentially identical to the original gas generator arrangement with two noteworthy exceptions. First, the direct technique utilized the cooling loop exit temperature in place of the gas generator level sense to control the LN_2 flow. Second, and perhaps the only inherent disadvantage associated with the gas generator elimination, is the critical dependence of the cooling loop capacity on the supply reservoir pressure. Repeated testing of the sensor cooling system, varying both supply pressure and the total elapsed time in the initial cooldown mode indicated an optimum cooling rate - hold time condition could be obtained with a supply pressure of 23 psig. Figure 14 illustrates a number of critical cryosystem parameters using the direct cooling approach.

Component Failures

B. High Voltage Regulated Power Supply, Power Technology, Inc., Block Engineering Drawing No. 623377

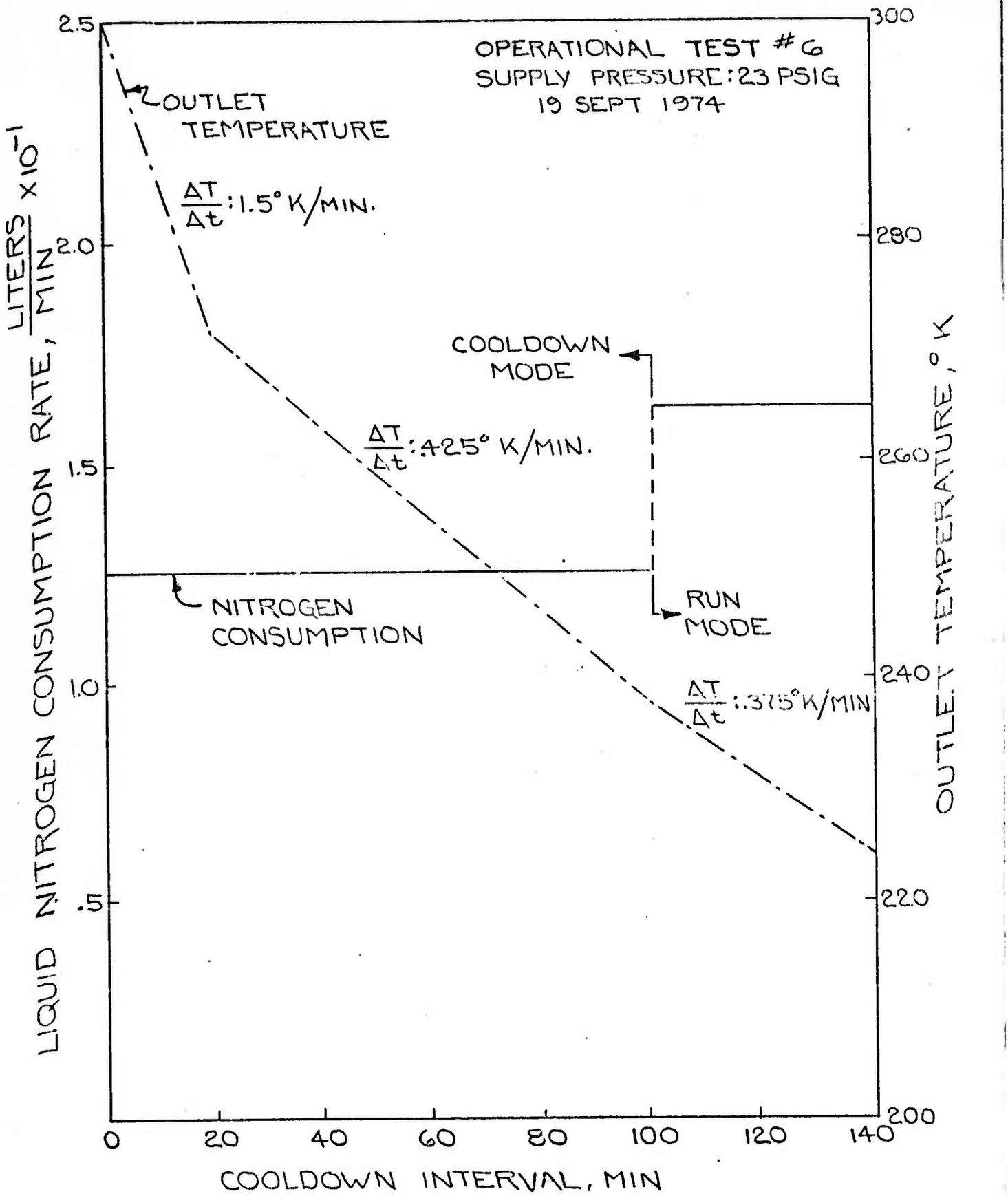

FIGURE 14

SENSOR COOLING CAPACITY

Description of Problem:

(1) Initial performance at room temperature and pressure - satisfactory

(2) In use exposure to low pressure (0.5 psig) - catastrophic failure

Failure Analysis and Corrective Action:

(1) Failure mechanism identified as device breakdown due to corona discharge

(2) Discussions with the vendor indicated a component packaging problem existed internal to the supply due in part to the additional nonstandard filtering required for this particular supply

(3) Unit returned to vendor for refurbishment and repackaging for low pressure operation as originally specified

Design Problem

A. Thermal loading on External Instrument Housing

Description of Problem:

(1) Conductive heat transfer via the housing lip cooled the external housing wall and the instrument top plate sufficiently for frost formation

Failure Analysis and Corrective Action

(1) Thermal analysis and retest indicated insufficient thermal isolation between the inner housing wall and the cooling coils. The reduced isolation overcame the action of the top plate heater allowing the temperature of all external surfaces to drop below the ambient dew point, a particular problem during sea level cooldown.

(2) Thermal loading of the top plate was minimized with the addition of a phenolic ring spacer between the housing and the top plate. Additional testing indicated a significant but not complete reduction condensation on the top plate. This residual moisture had no adverse effect on instrument operation.

Design Problem

B. Piezoelectric Fixed Mirror Adjust

Description of Problem:

(1) Arcing from piezoelectric elements to case a high voltage

Failure Analysis and Corrective Action:

(1) Arcing attributed to large voltage spikes across piezo elements if the adjustable voltage potentiometer was allowed to turn more than 300°, traversing a maximum/minimum voltage discontinuity.

(2) The problem was remedied with the addition of mechanical stops on the potentiometers, limiting the rotation

Design Problem

C. Bearing Assembly

Description of Problem:

(1) Excessive amount of energy necessary to reliably drive the moving mirror assembly

Failure Analysis and Corrective Action:

(1) Stiff operation of the bearing atributed to excess amounts of contamination and lubricant buildup on the outer bearing sleeve

(2) The mechanism was partially disassembled and cleaned of residue at the bearing ends. The static and dynamic characteristics of the bearing were not measured during this refurbishment due to the impracticality of a complete sensor disassembly and realignment.

(3) Subsequent operation of the instrument required a significantly reduced amount of energy to drive the moving mirror assembly.

SECTION VI

ACCEPTANCE TESTING

6.0 General

This section presents the results and conclusions of a series of tests and demonstrations performed by the contractor for the purposes of verifying conformance with certain performance requirements shown in the section entitled "Design Specifications". Testing was carried out in accordance with Block Engineering Acceptance Procedure, PNX-282002, identified as line item 003 of the Phoenix contract data requirements list.

6.1 Calibration

6.1.1 Field of View Measurement

The instrument field of view measurement was obtained with the interferometer drive disabled and the input energy on the detector modulated by a rotating chopper wheel. A continuous scan of the field in both azimuth and elevation directions was recorded and evaluated with the instrument at room temperature. The plot of the instrument field of view in the azimuth and elevation scans is shown in Figures 15 and 16 respectively. The plots indicate a circular field of view, 5.8 mr full angle, which is in good agreement with the design specifications.

6.1.2 Resolution Verification

The spectral resolution of the sensor was verified by evaluating computer processed spectra of a 3.39 μm HeNe laser source. Figure 17 reveals the unapodized 3.39 μm line profile with a measured frequency spread at one half the peak intensity equal to 0.64 cm^{-1}. Although this working resolution was within the design specification, the line profile was slightly broader

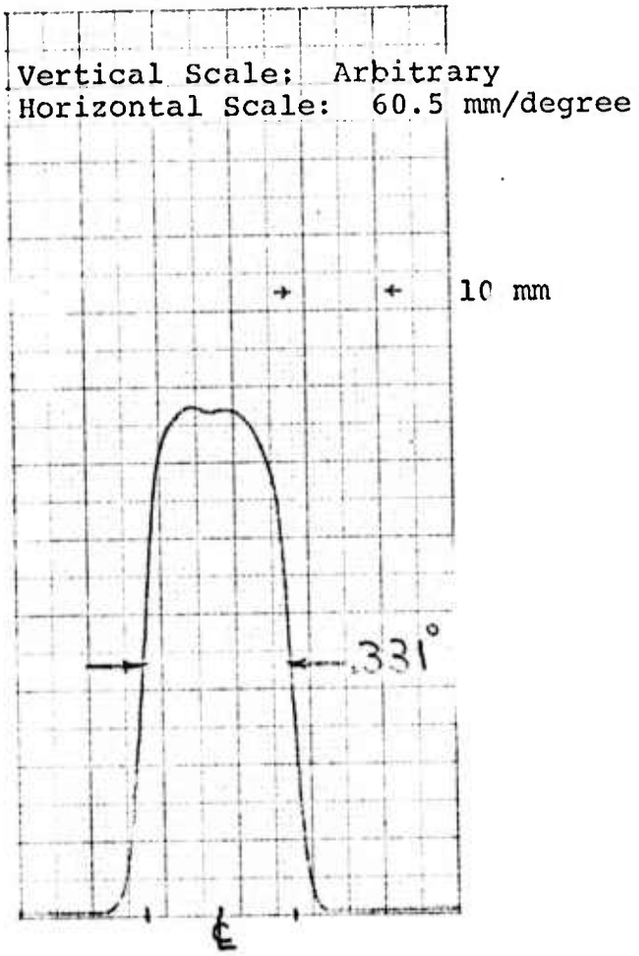

FIGURE 15

INSTRUMENT FIELD OF VIEW

AZIMUTH SCAN

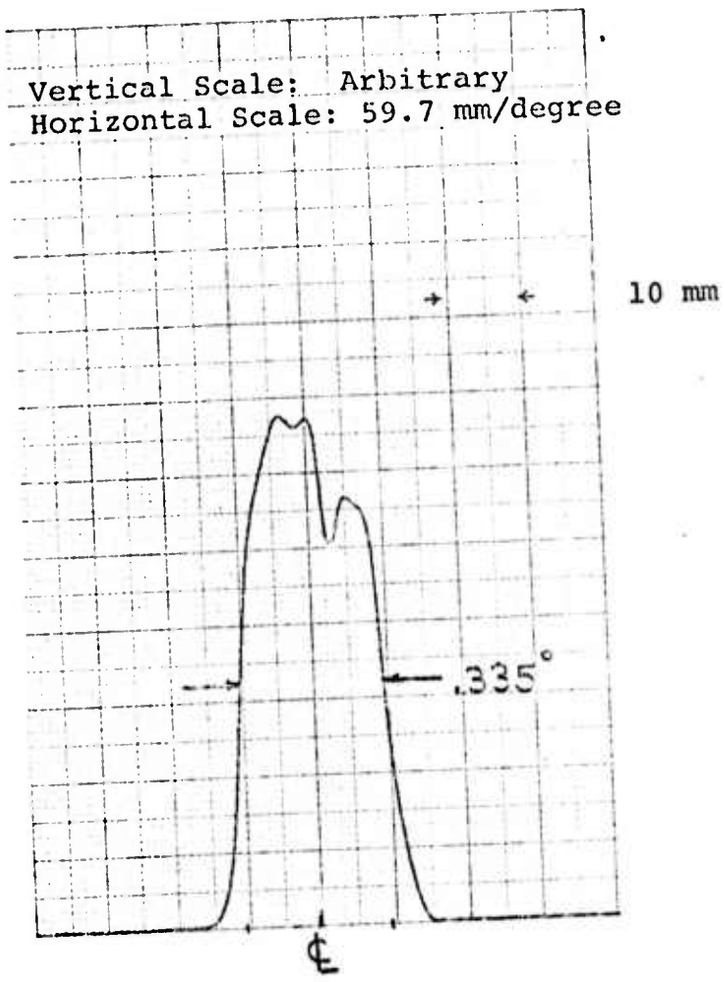

FIGURE 16

INSTRUMENT FIELD OF VIEW

ELEVATION SCAN

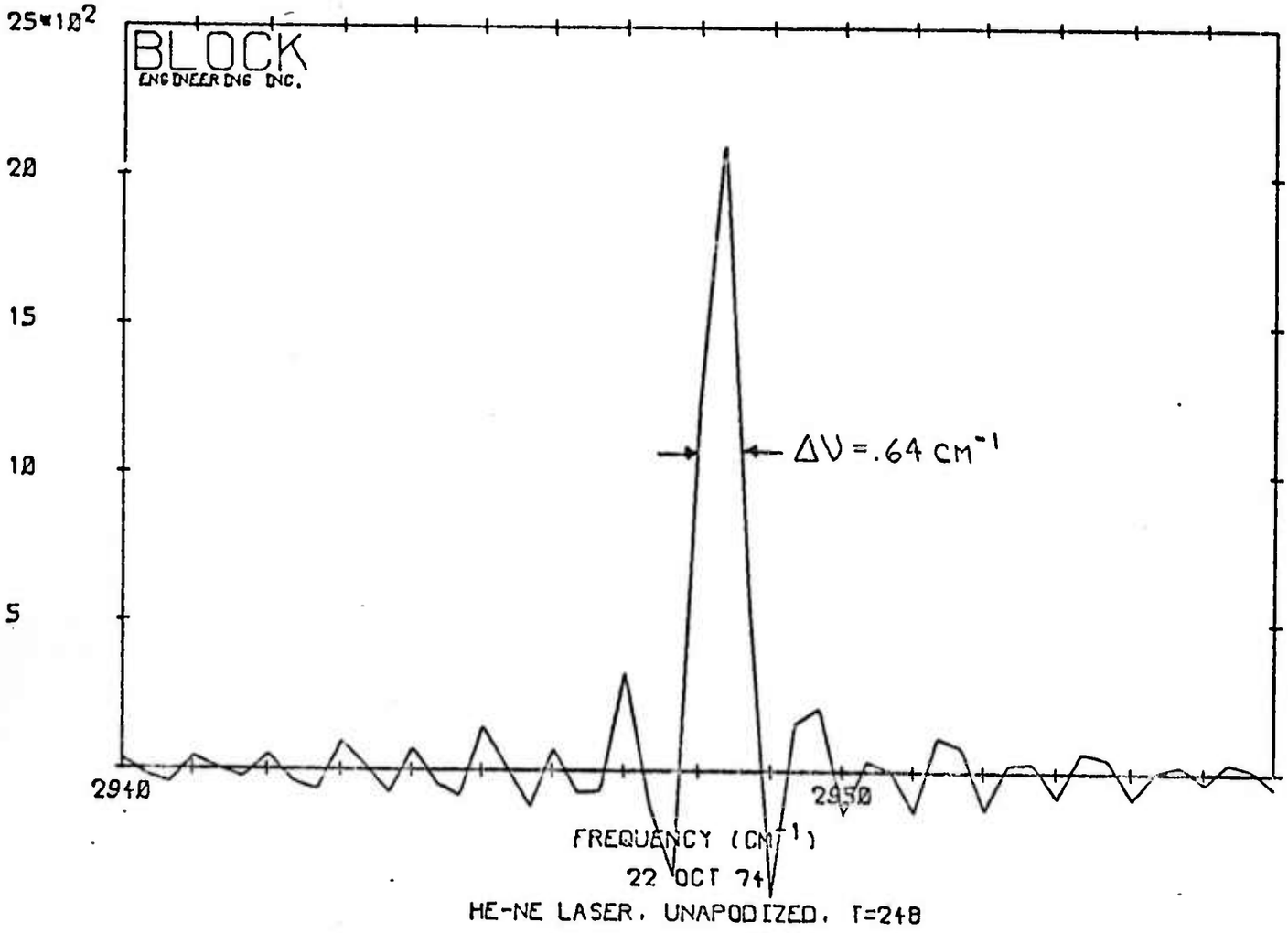

FIGURE 17

RESOLUTION VERIFICATION

than the expected resolution based upon the optical retardation of the instrument.

$$\Delta\nu \text{ (working resolution)} = \frac{3}{4} \times \frac{1}{B} = 0.48 \text{ cm}^{-1}$$

This anomaly was attributed to a bearing tilt factor in excess of 10 arc seconds present at the end of the stroke which produced an apodization of the monochromatic signal interferogram similar to a computer generated trapezoidal apodization function. As with any mathematic filtering process or apodization performed on the interferogram, regardless of origin, the spectral resolution will be degraded to some extent, becoming more pronounced at shorter wavelengths.

A subsequent investigation into the deterioration of the bearing performance during these calibration procedures concluded that a partial disassembly of the bearing mechanism during the operational checkout of the instrument was responsible for the change in dynamic operating characteristics of the bearing.

Figure 18 illustrates the working resolution of the sensor with the interferogram filtered with a computer generated triangular apodization function of the form

$$\Lambda = 1 - (|\delta|/L)$$

where

Λ = apodization function

δ = optical path difference, cm

L = maximum optical retardation, cm

As expected, the apodized spectra half peak line width was slightly broader at 0.87 cm^{-1} which is the anticipated result when one attempts to correct a monochromatic interferogram by

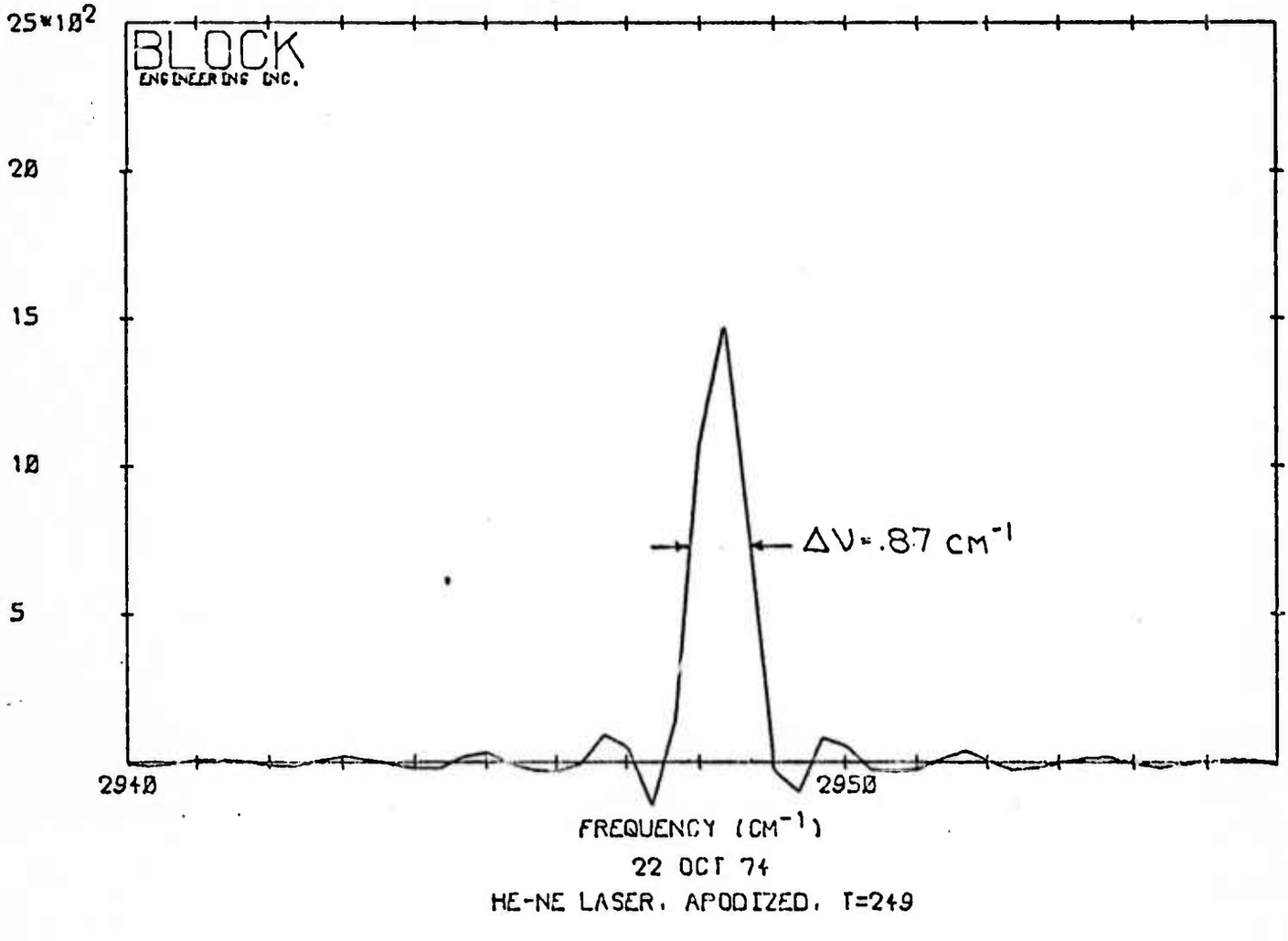

FIGURE 18

RESOLUTION VERIFICATION

multiplication with a triangular apodization function. A visual inspection of Figure 18 reveals that the apodized spectra closely approximates the ideal $sync^2$ transform of a monochromatic source with its reduced side lobes and smaller negative intensities.

6.1.3 Instrument Sensitivity

The predicted NESR (noise equivalent spectral radiance) of the sensor can be determined from the following relation

$$NESR = \frac{\sqrt{A_d}}{\eta\theta D^* \Delta\nu\sqrt{T}} = \frac{\sqrt{A_d}\ \sqrt{\Delta f}}{\eta\theta D^* \Delta\nu}$$

where

A_d = area of the detector, 7.8×10^{-3} cm^2

η = optical efficiency, 10^{-1}

θ = throughput, 2×10^{-3} cm^2-ster

$\Delta\nu$ = resolution, 0.64 cm^{-1}

T = integration time, 0.35 sec/scan

Δf = 1/T, 2.86 Hz

D^* = figure of merit, see discussion below.

As mentioned previously, see Table 2, the measured detector D^* using a simulated uniform 220°K background radiance was

$$D^*_{\lambda pk} = 3.63 \times 10^{11}\ cm\text{-}Hz^{\frac{1}{2}}\text{-}watt^{-1}$$

In practice, the detector experiences a background flux level somewhat higher than the 220°K test conditions due to the 250°K interferometer operation. As a result, the actual working detector D^* is predictably less than the above value. An accurate determination of the working D^* is obtained in the following manner. For a uniform 220°K background at altitude, the following photon flux is calculated

$$\Phi_{0\text{-}5.5\mu}(220°K) = 6.3 \times 10^{12} \text{ photons-sec}^{-1}$$

Now for a 220°K background with the interferometer operating at 250°K exhibiting a typical emissivity, ε, of 0.4

$$\Phi_{0\text{-}5.5\mu}(\text{working}) = \varepsilon \left[\Phi_{0\text{-}5.5\mu}(250°K)\right] + \left[1-\varepsilon\right] \left[\Phi_{0\text{-}5.5\mu}(220°K)\right]$$

$$= 1.58 \times 10^{13} \text{ photons-sec}^{-1}$$

The reduction in D* is expressed as the following ratio

$$\left[\frac{\Phi(220°K)}{\Phi(\text{working})}\right]^{\frac{1}{2}} = \left[\frac{6.3 \times 10^{12}}{1.58 \times 10^{13}}\right]^{\frac{1}{2}} = 0.63$$

or

$$D^*_{\lambda pk} = 2.28 \times 10^{11} \text{ cm-Hz}^{\frac{1}{2}}\text{-watt}^{-1}$$

Returning to the NESR calculation, $D^*_{\lambda pk}$ can now be converted to a spectral D^*_{λ} to obtain a predicted NESR at the wavelengths of interest

$$D^*(2\mu,1000,1) = 1.13 \times 10^{11} \text{ cm-Hz}^{\frac{1}{2}}\text{-watt}^{-1}$$

$$D^*(4\mu,1000,1) = 2.06 \times 10^{11} \text{ cm-Hz}^{\frac{1}{2}}\text{-watt}^{-1}$$

Substitution into the expression for sensitivity yields

$$\text{NESR}(2\mu) = 1.04 \times 10^{-8} \text{ watts/cm}^2\text{-ster-cm}^{-1}\text{-scan}$$

$$\text{NESR}(4\mu) = 5.7 \times 10^{-9} \text{ watts/cm}^2\text{-ster-cm}^{-1}\text{-scan}$$

The actual measured NESR of the instrument was determined from the computer processed spectra of a calibrated point

source blackbody. Numerically, the noise equivalent spectral radiance is equal to the ratio of the radiance to the rms signal to noise in the spectrum and was calculated by computing the theoretical blackbody irradiance at a particular temperature and wavelength and measuring the signal to noise from a plotted background corrected spectrum of an observed collimated point source blackbody of the same temperature. The sensitivity initially calculated as an NESI (noise equivalent spectral irradiance) was then divided by the solid angle field of view to obtain an NESR.

$$NESR = \frac{NESI}{\Omega} = \frac{H_{BB}(\lambda, 1000°K)}{S/N \times \Omega}$$

where

$H_{BB}(\lambda, 1000°K)$ = theoretical spectral irradiance, watts/cm^2-cm^{-1}

S/N = rms signal to noise ratio at the wavelength of interest, obtained from plotted spectra (see Figures 19-21)

Ω = solid angle field of view, ster

At 4 microns

$$NESR = 1.55 \times 10^{-8} \text{ watts/cm}^2\text{-ster-cm}^{-1}\text{-scan}$$

At 2 microns

$$NESR = 2.88 \times 10^{-8} \text{ watts/cm}^2\text{-ster-cm}^{-1}\text{-scan}$$

Both NESR values indicate the system sensitivity viewing a 300°K external background with the interferometer operating at 250°K. The actual improvement in sensitivity with a reduction in the external background temperature from 300°K to 220°K was determined from plotted noise data obtained

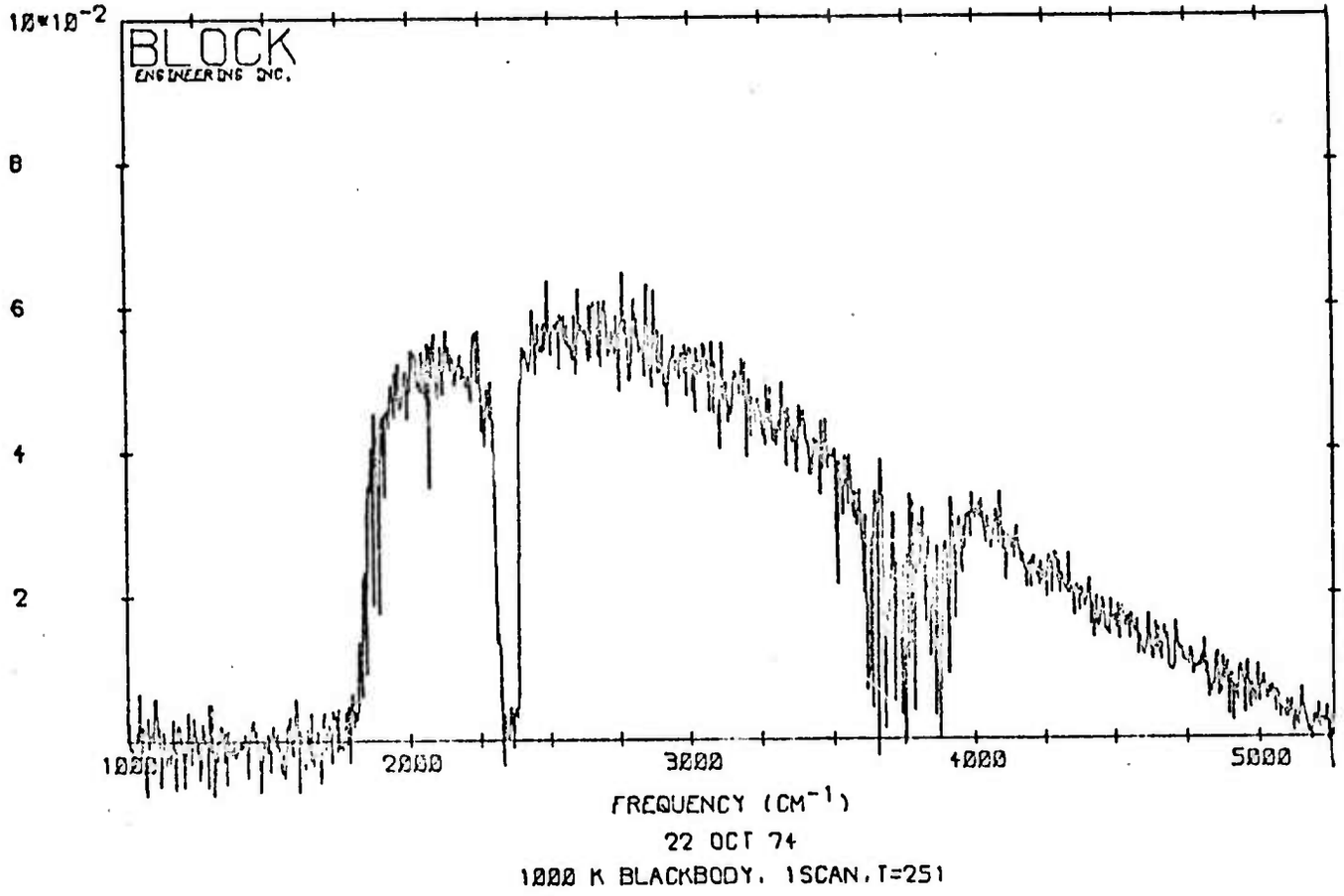

FIGURE 19

NESI VERIFICATION

BACKGROUND CORRECTED SPECTRUM

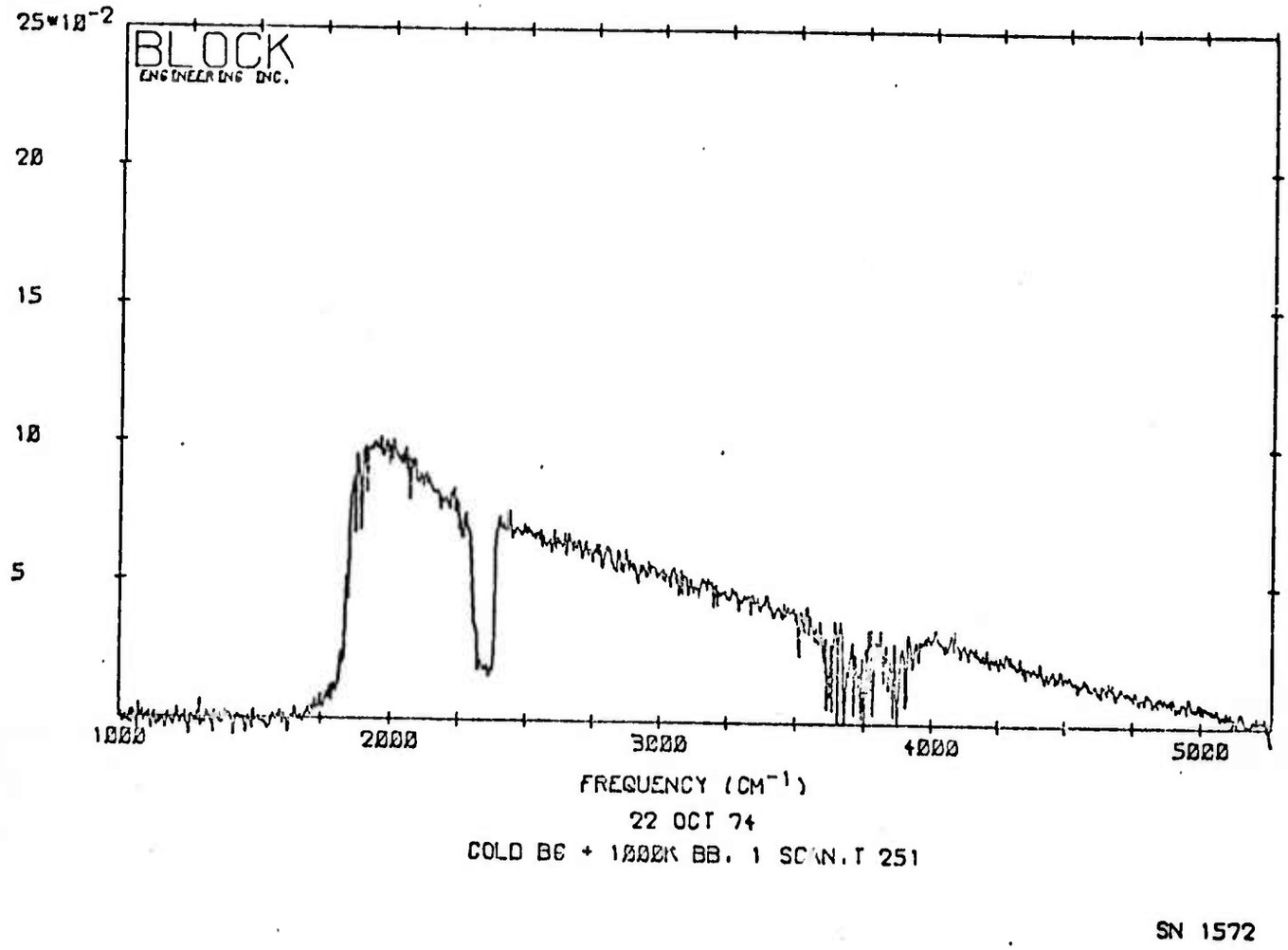

FIGURE 20

NESI VERIFICATION

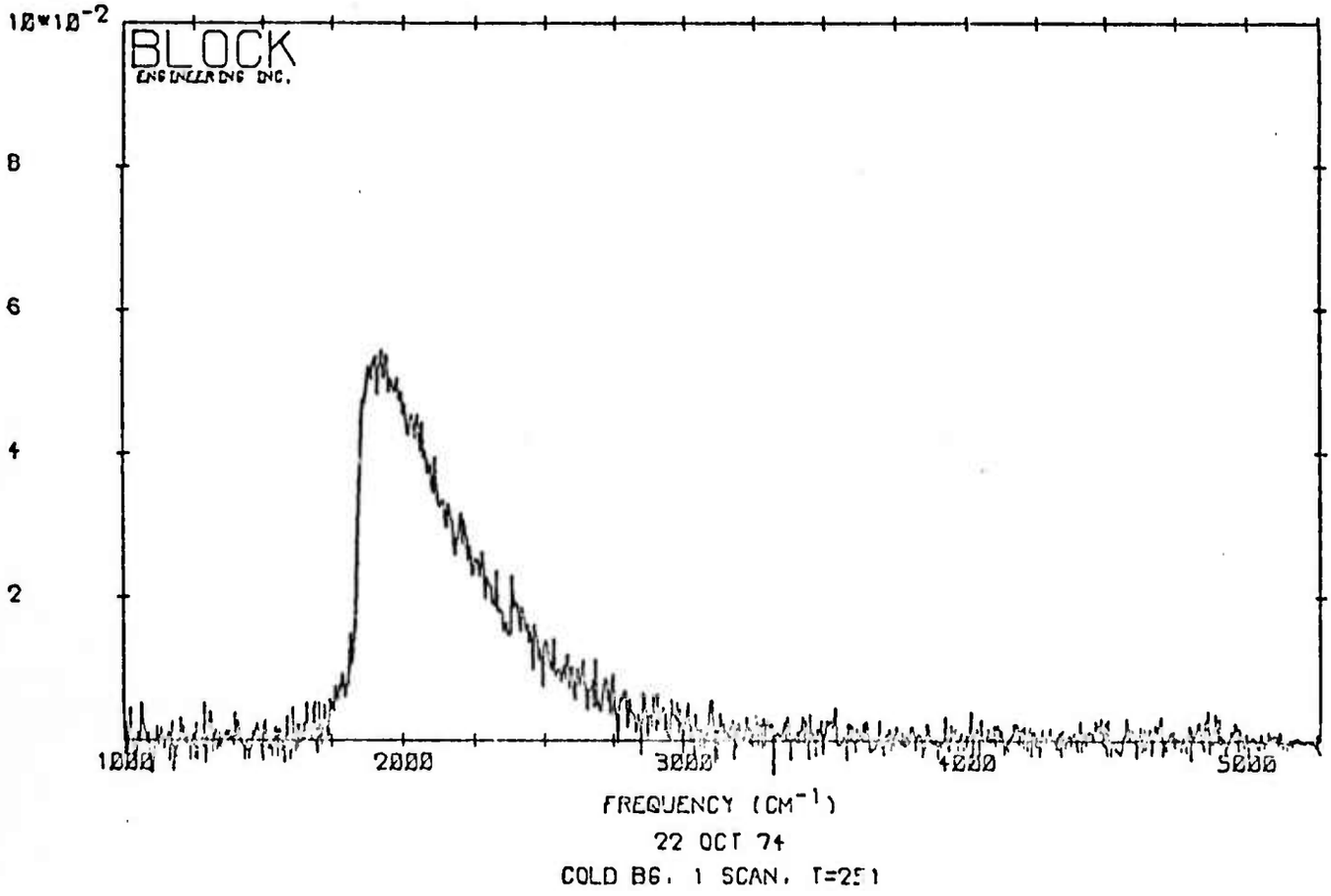

FIGURE 21

NESI VERIFICATION

during the environmental qualification of the instrument at Acton Environmental Laboratory, Inc., Acton, Mass. Figure 22 shows the normalized noise in the spectrum with the instrument viewing a 300°K external background. Figure 23 shows the normalized noise in the spectrum with the instrument operating at 250°K viewing a cold, 218°K external surface. A comparison of the "average" peak to peak noise in each spectrum shows a reduction in noise, hence an improvement in sensitivity by a factor of 2.3, therefore

$$\text{NESR } (4\mu, 220°K \text{ ext bkgd}) = 6.7 \times 10^{-9} \text{ watts/cm}^2\text{-ster-cm}^{-1}\text{-scan}$$

$$\text{NESR } (2\mu, 220°K \text{ ext bkgd}) = 1.2 \times 10^{-8} \text{ watts/cm}^2\text{-ster-cm}^{-1}\text{-scan}$$

These values, although in good agreement with the predicted result based on the measured D*, fall somewhat short of the following design constraints

$$\text{NESR } (4\mu) = 2 \times 10^{-9} \text{ watts/cm}^2\text{-ster-cm}^{-1}\text{-scan}$$

$$\text{NESR } (2\mu) = 4 \times 10^{-9} \text{ watts/cm}^2\text{-ster-cm}^{-1}\text{-scan}$$

Analysis of the compiled sensor test data attributed the failure to meet NESR requirements to the observed low detector sensitivity improvement at 220°K background (see Table 2). The tabulated results indicate an improvement factor of 2.1 currently exists with the Phoenix detector, significantly less than the 5.9 improvement factor predicted by photon flux reduction. This anomaly, further supported by a comparison of the noise spectra in Figures 22 and 2[illegible] is due primarily to significant internal noise mechanisms within the detector, particularly 1/f dependent noise, which become dominant at low background limiting sensitivity improvement.

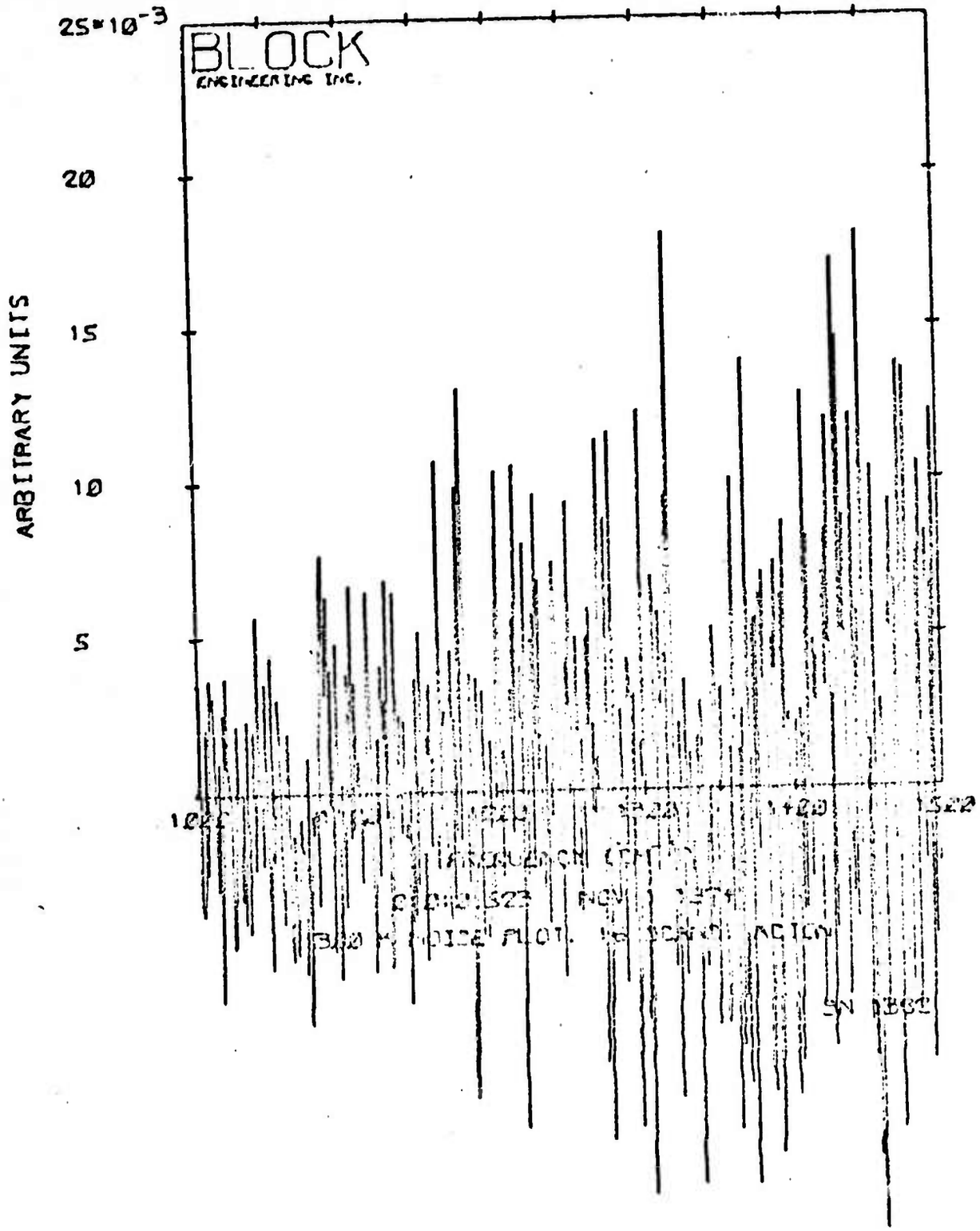

FIGURE 22

300°K NOISE PLOT - 16 SCANS

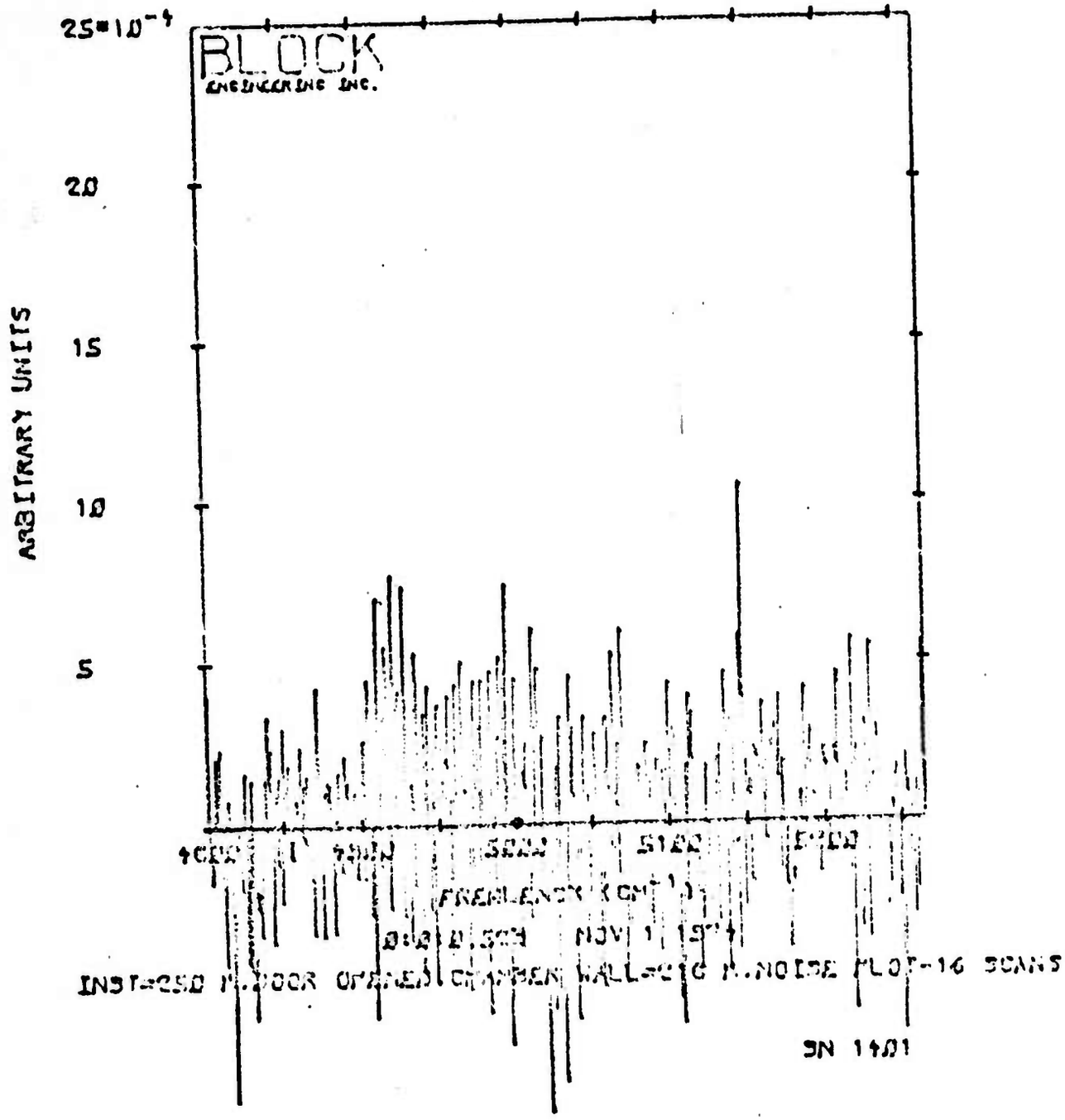

FIGURE 23

NOISE PLOT - INST = 250°K, DOOR OPEN VIEWING

TEST CHAMBER WALL = 218°K - 16 SCANS

It should be noted that the measured system sensitivity was obtained without spectral range reduction using the designed cold filtering capability. As mentioned previously, with the filter inserted a significant improvement in sensitivity was expected. However, due to the predominant detector noise under reduced background conditions, this improvement is unlikely to be realized.

6.1.4 Spectral Range Verification

The spectral range of the sensor without the cold filter was verified to be 2 - 5.5 microns via examination of the plotted 1000°K blackbody spectrum shown in Figure 20.

6.2 Environmental Qualification

The environmental qualification of the Phoenix system consisted of extended operation of the optical head in a simulated high altitude environment of 80,000 feet. The tests were conducted at Acton Environmental Laboratory, Inc. All systems were functionally verified as operating properly with the exception of the reference laser high voltage power; see Section 5.1 "Major Problem and Corrective Action" for a detailed discussion of the problems encountered.